

1 **Long-term chemical characterization of tropical and marine**
2 **aerosols at the CVAO: Field studies (2007 to 2011)**

3

4 **Khanneh Wadinga Fomba, Konrad Müller, Dominik van Pinxteren, Laurent**
5 **Poulain, Manuela van Pinxteren and Hartmut Herrmann**

6 TROPOS – Leibniz Institute for Tropospheric Research, Permoserstr. 15, 04318 Leipzig,
7 Germany

8 Corresponding author: Hartmut Herrmann (herrmann@tropos.de)

9

10

11 **Abstract**

12 The first long-term aerosol sampling and chemical characterization results from measurements at
13 the Cape Verde Atmospheric Observatory (CVAO) on the island of São Vicente are presented
14 and are discussed with respect to air mass origin and seasonal trends. In total 671 samples were
15 collected using a high volume PM₁₀ sampler on quartz fiber filters from January 2007 to
16 December 2011. The samples were analyzed for their aerosol chemical composition including
17 their ionic and organic constituents. Back trajectory analyses showed that the aerosol at CVAO
18 was strongly influenced by emissions from Europe and Africa with the later often responsible for
19 high mineral dust loading. Sea salt and mineral dust dominated the aerosol mass and made up in
20 total about 80% of the aerosol mass. The 5 year PM₁₀ mean was $47.1 \pm 55.5 \mu\text{g}/\text{m}^3$ while the
21 mineral dust and sea salt means were $27.9 \pm 48.7 \mu\text{g}/\text{m}^3$ and $11.1 \pm 5.5 \mu\text{g}/\text{m}^3$, respectively. Non-
22 sea-salt (nss) sulfate made up 62 % of the total sulfate and originated from both long range
23 transport from Africa or Europe and marine sources. Strong seasonal variation was observed for
24 the aerosol components. While nitrate showed no clear seasonal variation with an annual mean of
25 $1.1 \pm 0.6 \mu\text{g}/\text{m}^3$, the aerosol mass, OC and EC, showed strong winter maxima due to strong
26 influence of African air mass inflow. Additionally during summer, elevated concentrations of
27 OM were observed originating from marine emissions. A summer maximum was observed for
28 non-sea-salt sulfate and was connected to periods when air mass inflow was predominantly of

29 marine origin indicating that marine biogenic emissions were a significant source. Ammonium
30 showed a distinct maximum in spring and coincided with ocean surface water chlorophyll *a*
31 concentrations. Good correlations were also observed between nss-sulfate and oxalate during the
32 summer and winter seasons indicating a likely photochemical in-cloud processing of the marine
33 and anthropogenic precursors of these species. High temporal variability was observed in both
34 chloride and bromide depletion differing significantly within the seasons, air mass history and
35 Saharan dust concentration. Chloride (bromide) depletion varied from $8.8 \pm 8.5\%$ ($62 \pm 42\%$) in
36 Saharan dust dominated air mass to $30 \pm 12\%$ ($87 \pm 11\%$) in polluted Europe air masses. During
37 summer, bromide depletion often reached 100 % in marine as well as in polluted continental
38 samples. In addition to the influence of the aerosol acidic components, photochemistry was one
39 of the main drivers of halogenide depletion during the summer while during dust events,
40 displacement reaction with nitric acid was found to be the dominant mechanism. PMF analysis
41 identified three major aerosol sources including sea salt, aged sea salt and long range transport.
42 The ionic budget was dominated by the first two of these factors while the long range transport
43 factor could only account for about 14 % of the total observed ionic mass.

44 **Key words:** PM₁₀ aerosol, seasonality, chemical composition, Saharan dust, halogenide
45 depletion

46

47

48

49

50

51

52

53

54

55

56

57 **1. Introduction**

58 The interest in research on atmospheric aerosols is not only limited to heavily polluted megacities
59 and other strongly anthropogenically polluted areas but also concerns naturally mobilized dust
60 and sea-salt aerosols which are in the focus of marine chemistry, biology and atmospheric
61 chemistry (Raes et al. 2010; Radhi et al. 2010; Heller and Croot 2011; Formenti et al. 2011;
62 Carpenter et al. 2004; Quinn and Bates 2005). The creation and operation of the Cape Verde
63 Atmospheric Observatory (Observatório Atmosferico de Cabo Verde: Humberto Duarte
64 Fonseca, CVAO) located at the São Vicente island in 2006 was a joint activity of British, German
65 and Cape Verdean scientific institutes with funding from the European Union (EU), national
66 scientific projects and institutions. On the one hand, the CVAO is downwind of the Mauritanian
67 coastal upwelling region off northwest Africa, an area of high marine biological productivity.
68 Observations made at the CVAO therefore provide information on links between atmospheric
69 compositional changes, marine biology and climate. On the other hand, satellite, ground-based,
70 ship and aircraft measurements have shown the outflow of Saharan dust into the Atlantic Ocean
71 usually across the Cape Verde islands (Chiapello et al. 1999; Formenti et al. 2003; Reid et al.
72 2003; Tesche et al. 2011; Gelado-Caballero et al. 2012), making it a suitable location for
73 characterizing mineral dust. The station is situated at the far edge of the island in the direction of
74 air mass inflow to the island so that air masses observed at the station are free from local
75 pollution thereby making the station suitable for also performing remote marine aerosol
76 experiments. The atmospheric deposition of nutrients that are derived from dust such as nitrogen,
77 phosphorus and iron compounds into the oceans plays a crucial role in marine biogeochemical
78 cycles and in some areas establishes a major nutrient input to the open oceans (Cropp et al. 2005;
79 Ohde and Siegel 2010; Bates et al. 2001). The role of desert aerosols in atmospheric processes
80 strongly depends on a variety of physicochemical parameters and their spatial distribution and
81 transformations in the atmosphere (Kandler et al. 2007; Kelly et al. 2007).
82 During late spring and summer, the CVAO site mostly receives North Atlantic marine air masses
83 along the NNE trade winds which, although, are sometimes influenced by the Mauritanian
84 upwelling, provide the possibility for long-term studies of “background” Atlantic air and its
85 associated trace gases of oceanic origin. During late fall and winter, Cape Verde is situated in the
86 direct transport pathway of Saharan dust from Africa to the North Atlantic. During this season
87 dust is transported in the lower troposphere and the deposition takes place mainly over the eastern

88 tropical Atlantic (Schepanski et al. 2009) and Cape Verde.
89 In principle, atmospheric chemistry in this region of the Cape Verde Islands is expected to be
90 influenced by emissions from the ocean (Mahajan et al. 2010; Read et al. 2008), Saharan dust,
91 anthropogenically released gases and particles from continental Africa, south-western Europe and
92 in minor cases North-American sources.
93 The investigation of the role of mineral dust in the ocean has been the focus of a number of
94 research and ship cruises along the tropical Atlantic oceans (Bates et al. 2001; Chen and Siefert
95 2003; Allan et al. 2009). However, these measurements have mostly focused on short term
96 measurements during intensive field campaigns that last for 3-6 weeks, making predictions about
97 seasonal variability and long term understanding of atmospheric processes quite difficult. Such
98 long-term data sets have been often requested (Mahowald et al. 2005) but only a few data
99 actually exist for the region of the tropical North Atlantic (e.g., Kandler et al. 2007; Chiapello et
100 al. 1995). Chiapello et al. (1995) collected filter samples over three years for metal analyses at the
101 Cape Verde island Sal from a region that was far from the coastline and influenced by the island
102 itself. There are also some data from ship cruises and short term experiments near this region
103 (Kandler et al. 2007; Chen and Siefert 2004; Rijkenberg et al. 2008). Long-term observations
104 were made in the subtropical region at Izaña (Tenerife) 1500 km NNE from São Vicente but
105 Izaña is located at 2373 m a.s.l. and Santa Cruz is influenced heavily by local pollution (Alastuey
106 et al. 2005). Remote site long-term measurements in the north-eastern tropical Atlantic Ocean are
107 not known. In a recent study by Schulz et al. (2012), a marine atmospheric monitoring network
108 for long-term observations of dust transport and deposition to the ocean was asked for as well as
109 encouraged for future harmonized activities in marine aerosol research. The measurements at the
110 CVAO intend to improve on the present data scarcity and also meet other expectations.
111 Within the present study the long-term PM_{10} high volume filter measurements taken at the
112 CVAO are discussed. The presented results aim to deliver the first long-term data set of aerosol
113 chemical composition for further use, e.g. in marine biogeochemistry research and for marine
114 aerosol modeling where long-term experimental data on the aerosol constitution and its size-
115 resolved chemical composition are needed. The results are focused on samples collected since the
116 creation of the CVAO in 2007 until the end of 2011. The aspects addressed are particulate mass
117 concentrations, chloride depletion, concentration of ionic components, organic matter (OM) and
118 elemental carbon (EC). The mineral dust fraction of the aerosol particles and its seasonal and
119 inter-annual variability are also discussed. Back trajectories were used to classify typical source

120 regions. Related works from the CVAO includes first investigations from short term experiments
121 of PM characterization (Müller et al., 2010, Fomba et al., 2013) and of specific organic single
122 compounds Müller et al. (2009).

123

124 **2. Experimental**

125 **2.1 Site and sampling**

126 Sampling was done at the CVAO which is located at the north-eastern shore of the island of São
127 Vicente in Cape Verde. The sampling site is situated 70 m from the coastline ($16^{\circ} 51' 49''$ N, 24°
128 $52' 02''$ W, about 10 m a.s.l.). This region experiences constant north-eastern winds from Africa
129 through the Canary Islands. The average annual temperature at the CVAO is $23.6 \pm 4.0^{\circ}\text{C}$ and it
130 is an arid region with a maximum of 24-350 mm rainfall per year. The precipitation frequency is
131 about 3 to 10 events per year mainly between August and October. Therefore, the wet deposition
132 of particles in this region is negligible. A more detailed description of the meteorological
133 conditions can be found in Carpenter et al. (2010). Sample collection was performed on top of a
134 tower with an inlet height of 32 m to reduce the direct influence of sea spray on the collected
135 particles. Due to the location of the station, influences from the island like orographic influences
136 in dust sedimentation and anthropogenic emissions are negligible. Thus the collected samples are
137 representative of a clean atmosphere over the ocean and not contaminated by gases or particulates
138 from the island itself. However, though such events are very rare, during southwesterly winds
139 influences from the island could be observed.

140 All background meteorological data, temperature, relative humidity, and wind measurements
141 were collected from 31 m and from 10 m heights at a frequency of 1 Hz, then averaged over one
142 minute and ten minutes to hourly values. Atmospheric pressure and broadband UV radiation were
143 recorded at a 4 m height.

144 Particle sampling was done using a high volume (HV) collector with a PM_{10} -inlet (Digitel filter
145 sampler DHA-80, Walter Riemer Messtechnik, Germany) that was operated with an average flow
146 rate of 500 l/min in a 24 h sampling period during intensive campaigns and was switched to 72 h
147 sampling period, otherwise. The high volume samples were collected on acquired 150 mm pre-
148 heated quartz fiber filters (Munktell, MK 360) and were further pre-heated in our laboratory at
149 110°C for 24 h to get rid of the OC background content. Our unpublished results of tests at

150 higher temperatures delivered similar blanks but the mechanical stability of the filters (abrasion
151 and breaking resistance) was better when handling at 110°C.

152 After sampling the filters were stored at 5 °C and subsequently cooled and transported to a
153 freezer. The long term storage and transportation of the collected filters from the CVAO to
154 Germany was always carried out in aluminum boxes at -20 °C.

155

156 **2.2 Laboratory Analysis**

157 The filters were equilibrated for 72 h under constant temperature (20 ± 1 °C) and humidity (50 ±
158 5%) before and after collection and weighed using a microbalance (Mod. AT261 Delta Range,
159 Mettler-Toledo, Switzerland) with a reading precision of 10 µg.

160 For ion analysis, 25 % of the PM₁₀ quartz fiber filter was extracted with 30 ml MilliQ-water
161 (>18 MΩ cm, 15 min shaker, 15 min ultrasonic bath, 15 min shaker). Sample extracts were
162 filtered through a 0.45 µm one-way syringe filter to remove insoluble materials prior to ion
163 analysis. Ion analysis was performed for cations Na⁺, NH₄⁺, K⁺, Mg²⁺, Ca²⁺ and anions Cl⁻, Br⁻,
164 NO₃⁻, SO₄²⁻ and C₂O₄²⁻ using a standard ion-chromatography technique (ICS3000, DIONEX,
165 USA) equipped with an automatic eluent generation (KOH for anions and methanesulfonic acid
166 (MSA) for cations) and a micro-membrane suppression unit. For the anion separation a
167 combination of AG18 and AS18 (2 mm) was applied while for the cation separation CG16 and
168 CS16 (3 mm) were used. Chromatographic calibrations were carried out daily using a four point
169 standard (Fluka, Switzerland). The detection limits for all ions measured by conductivity
170 detection were within 0.002 µg/m³ except for calcium that was 0.02 µg/m³. Bromide was detected
171 using UV/VIS detection (VWD-1, Dionex) with a detection limit of 0.001 µg/m³. Analyzed field
172 blank filters were used for blank correction via subtraction. Non-sea salt sulfate (nss-sulfate) was
173 determined from the subtraction of sea salt sulfate (ss-sulfate) from the total sulfate. Ss-sulfate
174 was determined from the stable ratio SO₄²⁻/Na⁺=0.251 (Liebezeit, 2011) in sea water under the
175 assumption that sodium has no other sources.

176 Organic and elemental carbon were analyzed by a two-step thermographic method (C-mat 5500,
177 Ströhlein, Germany) with NDIR detection as described in the following literatures (Gnauk et al.
178 2008; Neusüss et al. 2002; Carpenter et al. 2010). The detection limits for quartz fiber filter
179 analysis were 30 ng/m³ for EC and 100 ng/m³ for OC. For the determination of OM (organic
180 matter) the estimation of Turpin (Turpin et al. 2000) was applied with OM considered as twice

181 OC (OM = OC * 2) which is recommended for aged aerosols. In previous studies, results of
182 single organic compounds were presented (Müller et al. 2009; Müller et al. 2010) while in the
183 present work, only oxalic acid concentrations shall be discussed.

184 Air mass back trajectory analyses were performed to assist in the data interpretation and to
185 provide useful hints on various air mass origins. Back trajectories ensembles (van Pinxteren et al.
186 2010) were calculated (starting 500m above ground) using the NOAA HYSPLIT (HYbrid Single-
187 Particle Lagrangian Integrated Trajectory, <http://www.arl.noaa.gov/ready/hysplit4.html>) model.

188

189 **2.3 Positive Matrix Factorization (PMF) Analysis**

190 Source apportionment of the analyzed aerosol chemical composition (OC, EC, Na^+ , NH_4^+ , K^+ ,
191 Mg^{2+} , Ca^{2+} , Cl^- , Br^- , NO_3^- , SO_4^{2-} and $\text{C}_2\text{O}_4^{2-}$) was performed using the multilinear Engine
192 algorithm (ME-2) developed by (Paatero 1999)). Results were analyzed according to the ME-2
193 graphic interphase Sofi from (Canonaco et al. 2013)). Since PMF is a weighted least square
194 method, individual estimates of uncertainties associated with each data value are required. In this
195 work the uncertainties were obtained from the calibration uncertainties of the main ions and
196 OC/EC that were applied on the measured concentrations. The PMF was run using 2 to 5 factors
197 and each factor solution was evaluated using the seed. It was found that the 3 factors solution
198 could explain the data most appropriately and thus provided the most meaningful results (Figure
199 SI-2 in the supplementary information). The obtained solution was interpreted on the basis of the
200 air mass back trajectories, the meteorological conditions and the chemical composition of the
201 filters. Further details on the results of the different factors could be found in the supplementary
202 information (SI).

203

204 **3. Results**

205 **3.1 Back trajectory analysis**

206

207 *Please insert Figure 1 here*

208

209 Hourly back trajectory analyses were performed for more than 600 samples. In general, 96 h back

210 trajectory ensembles were calculated. The plots represent a trajectory ensemble consisting of 648
211 single back trajectories calculated for a 24 hour time interval of the individual samples. For a few
212 sampling periods longer back trajectories were calculated for a better understanding of possible
213 sources since submicron particles could have longer atmospheric lifetimes (Jaenicke 1980)
214 depending on the height (Williams et al. 2002). The most important air mass origins were
215 classified as follows (Fig. 1):

216 (A) The air mass spent the last 96 h over the Atlantic Ocean and was from the northern or
217 northwestern Atlantic Ocean (16.5 % of all samples).

218 (B) The air mass spent less than 48 h over the Ocean in the last 96 hours before arriving at
219 CVAO and originated from the African continent crossing over the Saharan Desert, urban sites
220 (Nouakchott, Dakar, etc.) as well as biomass burning regions through the Mauritanian upwelling
221 region to the CVAO (22.2 % of all samples).

222 (C) Air masses from the Atlantic Ocean crossing the Mauritanian upwelling region, partially NW
223 Africa, Canary Islands (26.3 % of all samples).

224 (D) Air masses which originated from or in SW Europe and crossed the Mauritanian upwelling
225 region, coastal areas in NW Africa and/or the Canary Islands and the north-eastern Atlantic
226 Ocean (17.7 % of all samples).

227 (E) All further back trajectories (17.3 % of all samples) that could not be assigned to the above
228 four major classes. This include air masses that reached the CVAO from western Africa (south of
229 the Sahara), the equatorial Atlantic Ocean and from North-America.

230 Late fall and winter are the typical dust seasons at the Cape Verde islands. During this time
231 easterly and northeasterly winds transport Saharan dust into the tropical eastern Atlantic. During
232 spring and summer, the air mass origin is mainly marine but sometimes the trade winds cross the
233 African coast in Morocco and Western Sahara and at times originate from the Iberian Peninsula.
234 Equatorial air masses rarely reach the Cape Verde archipelago.

235 **3.2 Chemical characterization of the aerosol constituents**

236 671 samples were collected and analyzed for their chemical composition over the stated time
237 period. Table 1 shows the overview of the total number of investigated samples in this work
238 during the investigated time period. The observed difference in the number of collected filters
239 between the years is related to the different sampling routines that were implemented. During the
240 first four months of sampling in 2007, the samples were collected as 72 hours samples within one

241 week in the regime 3 h sampling and 4 h sampling break. After the first intensive campaign
242 (May/June 2007) during which sample collection was done for 24 h without a break between
243 filter sampling, the collection was changed to 3 days continuous sampling and 3 days pause
244 within the time period of August 2007 and December 2008. Afterwards the sampling period was
245 fixed at 72 h without a break. A few exceptions to this sampling regime were caused by power
246 failures at the CVAO and sampler defect in July/August 2009 (cf. Table 1). This explains the
247 higher number of filters observed in 2009 to 2011 in comparison to 2007 and 2008. From
248 October 2009 to July 2010 samples were collected on top of a container due to the reconstruction
249 of the tower. At the lower sampling height (4 m) the direct sea spray from the nearby coastline
250 influenced the aerosol constitution enormously. In these samples the sea-salt concentration was
251 about four to five times higher than in samples collected from the top of the tower.

252

253 *Please insert Table 1 here*

254

255 ***Mineral dust estimation and marine aerosol***

256 The estimation of the mineral dust content in the aerosol samples was achieved by the subtraction
257 of all determined species including the estimated mass of water, from the total mass. This was
258 done as a first approximation since major mineral dust component such as Al, Si or Fe were not
259 measured due to technical reasons. Thus, the mineral dust assumed here is analogous to the rest
260 of the undetermined aerosol component and is thus considered as the maximum possible dust
261 concentrations. The water content of the samples was estimated via the E-AIM model III of
262 Clegg et al. (1998). This model, however, delivers higher water content values than the
263 application of a hydration multiplication factor of 1.29 to the mass of all water soluble inorganic
264 compounds as suggested by Harrison et al. (2003) and Sciare et al. (2005). Using Clegg's model,
265 the average aerosol water concentration was $5.7 \pm 3.4 \mu\text{g}/\text{m}^3$. The uncertainty obtained due to the
266 application of this model was less than 10% ($0.5 \mu\text{g}/\text{m}^3$) in the estimated water content. The
267 estimated error had negligible effect on the estimated dust concentrations since the value was far
268 small compared to the uncertainty related to the determination of the other measured ions.
269 Mineral dust which in this region was mostly Saharan dust was the most dominant component of
270 the particulate matter, with a five-year average of $25.8 \pm 51.1 \mu\text{g}/\text{m}^3$ equivalent to about 55 % of
271 the total average aerosol mass concentration. Strong temporal and seasonal variations were
272 observed for the dust concentrations with concentration ranging from zero to $575.6 \mu\text{g}/\text{m}^3$.

273 The highest dust concentration was found during the winter season due to frequent Saharan dust
274 events that were strongly influenced by the Harmattan, a characteristic wind transporting Saharan
275 dust in lower heights to the Atlantic Ocean between the end of November and the beginning of
276 March. A few heavy dust events were observed in spring and fall but not in the summer. In
277 general, differences were found in the aerosol chemical composition during days of and days
278 without dust storms.

279 The mean aerosol composition of Saharan dust dominated samples corresponding to aerosol mass
280 concentrations higher than 90 $\mu\text{g}/\text{m}^3$ and that of marine aerosol dominated days with aerosol
281 mass less than 20 $\mu\text{g}/\text{m}^3$ is shown in Figure 2. Both situations had same chemical components
282 including, water soluble ions, organic and elemental carbon, water and mineral dust, with
283 different fractional composition. As would be expected aerosol water was lower during dust
284 storms than during marine influenced days. Sea salt concentrations did not change significantly
285 during and without dust storms. However, the relative contribution of sea salt was higher in
286 marine influenced air masses than in Saharan dust air masses.

287

288 *Please insert Figure 2 here*

289

290 Higher concentrations were also observed for sulfate, nitrate, EC/OM, and the crustal elements
291 such as potassium and calcium during dust events as compared to marine influenced days.
292 However, their relative compositions during dust events were lower than during marine
293 influenced days due to the total absolute mass. During non-dust period long range transport from
294 the northwestern African coast, Europe and secondarily formed PM from the ocean were the
295 main sources of nss-aerosol constituents.

296 *Please insert Table 2 here*

297

298 **3.3 Temporal and seasonal variations**

299 Results of the measured chemical components are shown in Table 2 including their 5 year
300 averages, minima and maxima. This is the first unique dataset of nearly continuously collected
301 PM from the Cape Verde archipelago and in the region of the northern tropical Atlantic over a
302 time period of five years. In the following, the temporal and seasonal variations of the PM
303 constituents are discussed with respect to the meteorological conditions and air mass origin.

304 Figure 3 shows the temporal trends of some of the investigated chemical components within the
305 stated time period. The red lines represent the time period during which sample collection was
306 performed on top of a container, while the blue lines represent measurements that were
307 performed on the 30 m tall tower.

308

309 *Please insert Figure 3 here*

310

311 **3.3.1 PM₁₀ mass concentration**

312 During the five years of PM collection at the 32 m sampling height an average mass
313 concentration of $47.1 \pm 55.5 \mu\text{g}/\text{m}^3$ was observed. Aerosol mass showed strong variability with
314 minimum and maximum values of $4.0 \mu\text{g}/\text{m}^3$ and $601.8 \mu\text{g}/\text{m}^3$, respectively (Table 2). The
315 highest and lowest daily mean concentrations were observed in January 2008 and March 2009,
316 respectively. Low concentrations were observed during days with low wind speeds of remote
317 Atlantic Ocean air mass inflow, and/or after precipitation events which typically occurred in the
318 fall. The highest aerosol mass was observed during days of Saharan dust storm when air mass
319 crossed the Saharan desert prior to their arrival at CVAO. Table 3 shows an overview of the mass
320 concentration of the number of samples sampled during different seasons. At the CVAO, particle
321 mass concentration was a good indication of the aerosol mineral dust content. Typically, mass
322 concentrations below $20 \mu\text{g}/\text{m}^3$ were observed during pure marine air mass inflow (Figure 1A).
323 When aerosol mass concentrations were between $20 \mu\text{g}/\text{m}^3$ and $90 \mu\text{g}/\text{m}^3$ the air mass originated
324 from any of the three above mentioned air mass classes C to E as shown in Figures 1B-D or also
325 of marine origin with higher wind speeds. The only exception was observed when the samples
326 were collected at a 4 m height, during which sea salt concentrations increased dramatically and
327 the above mentioned trends could not hold. The spikes in the PM₁₀ profile as shown in Figure 3,
328 corresponding to mass concentrations above $90 \mu\text{g}/\text{m}^3$ were indicative of days where aerosol
329 mass was dominated by Saharan dust (Figure 1B). On average, such strong Saharan dust events
330 were observed about 11-19 times a year. The duration of Saharan dust events varied from one to
331 ten days with the longest event also supported by back trajectory analysis observed from the 25th
332 of December 2007 to 4th of January 2008.

333

334 *Please insert Table 3 here*

335

336 In Figure 4, the inter-annual and seasonal variation of some chemical aerosol components is
337 presented. The inter-annual variation of the monthly mean of the PM₁₀ mass concentration is
338 shown in Figure 4. The highest mass loadings were observed in 2008 and the lowest in 2009. A
339 strong seasonal trend was found in the mass loadings. The average mass concentrations were
340 71.8 ± 34.3 , 33.7 ± 15.3 , 36.5 ± 10.3 and $43.7 \pm 12.6 \mu\text{g/m}^3$ for winter, spring, summer and fall,
341 respectively. The highest temporal variation was observed during the winter season due to
342 frequent change in air mass inflow. The lowest mass concentrations were observed in the spring
343 season (April to June) despite some episodic dust events during this period (e.g. May 2007) while
344 the highest concentrations were observed during the late fall and winter (December to February).
345 Similar seasonal trends were reported by (Chiapello et al. 1995) for the island of Sal despite their
346 more continental location on the island whereby anthropogenic activities could strongly affect
347 mass loadings. According to (Schepanski et al., 2009) the Sahara produces larger amount of dust
348 during summer but the dust is transported at higher altitudes of up to 10 km within the Sahara Air
349 Layer while in winter the dust is transported along the north-east trade winds at far lower
350 altitudes. Thus the higher amounts of Saharan dust, anthropogenically released gaseous and
351 particulate compounds from the African continent are responsible for the winter elevated PM₁₀
352 mass concentrations while marine and non-African air mass inflow were responsible for low
353 mass loadings.

354

355 *Please insert Figure 4 here*

356 **3.3.2 Sea salt**

357 Sea salt concentration was estimated as $1.17 * ([\text{Na}^+] + [\text{Cl}^-])$ (Anguelova, M. D, 2002). The
358 temporal variation of sea salt concentrations is shown in Figure 3. The observed concentration of
359 sea salt was strongly dependent on the meteorological conditions and the sampling height. The
360 averaged wind speed at the CVAO was about at 7.3 ms^{-1} while the maximum wind speed
361 observed was about 13 ms^{-1} . During days with high wind speeds the sea salt concentrations
362 increased strongly. The highest wind speeds were often combined with air masses coming from
363 North America crossing the northern Atlantic to CVAO. This observation was made after the
364 back trajectories analysis of and is valid for the majority of these events.

365 During such days, the aerosol mass was slightly higher than in days with lower ($< 4 \text{ ms}^{-1}$) wind
366 speed or dominant marine air mass inflow. The averaged sea salt concentration was 11.1 ± 5.5

367 $\mu\text{g}/\text{m}^3$ in samples collected on top of the tower and $58.3 \pm 28.3 \mu\text{g}/\text{m}^3$ for samples collected at the
368 4 m sampling height. Sea salt and other sea spray associated aerosol components increased
369 enormously (about a factor of 5) at the lower sampling height. This was due to the fact that
370 sample collection at 4 m height was done within the internal marine boundary layer (Niedermeier
371 et al. 2013) whereby aerosol mass was mostly affected by the surf zone. Increase in sea salt
372 concentrations were observed during days of high wind speeds but a strong correlation between
373 sea salt and the local wind speed was not observed. According to De Leeuw et al., (2000) and
374 Niedermeier et al., (2013), sea salt concentrations may increase significantly at wind speeds
375 above 10 ms^{-1} depending on the wind direction and the oceanic waves. The highest sea salt
376 concentration determined at the tower was $54 \mu\text{g}/\text{m}^3$ in spring 2011 in an episode when the local
377 wind speed was 13 ms^{-1} . The temporal variability of sea salt was not strong as compared to those
378 of mineral dust and aerosol mass. No seasonal trend was observed in the sea salt concentrations
379 and Mg/Na ratio found in the dust (0.12) and non-dust (0.11) samples was similar to the ratio in
380 sea salt (0.12), implying no influence of the dust storms on sea salt especially on sodium
381 concentration was observed.

382

383 **3.3.3 Sulfate**

384 Sulfate consisted of sea salt sulfate (ss-sulfate) and of non-sea salt sulfate (nss-sulfate) mainly of
385 secondary origin. In Figure 3, the temporal variability of the total sulfate concentration is
386 presented. Sea salt sulfate had a similar temporal trend as sea salt, thus, the variations observed in
387 the time series are attributed to variations in nss-sulfate concentration. On the average, ss-sulfate
388 made up only 38 % of the total sulfate measured at the tower. This, however, increased when
389 sampling was done at a lower height. The highest sulfate concentrations were strongly connected
390 to Saharan dust events but not all dust events were responsible for the elevated sulfate
391 concentrations. When air mass containing dust did not have contact with anthropogenic SO_2
392 pollution sources, the nss-sulfate was not elevated and vice versa. During the dust season marine
393 sources of nss-sulfate played a minor role. The averaged nss-sulfate concentration in winter
394 marine air masses was $0.47 \pm 0.31 \mu\text{g}/\text{m}^3$ while for the dust days the averaged nss-sulfate
395 concentration was $2.46 \pm 1.05 \mu\text{g}/\text{m}^3$. The strong increase in sulfate concentrations during the
396 dust events is indicative of anthropogenic activities in Africa that influences the aerosol
397 constitution. Natural sources of SO_2 are unlikely since the only nearby natural source is the ocean
398 and nss-sulfate secondary produced from oceanic precursors would therefore not vary

399 significantly with air mass origin. In Figure 4 the inter-annual and seasonal variation of nss-
400 sulfate is given. The average monthly concentration ranged from $0.43 \mu\text{g}/\text{m}^3$ to $3.0 \mu\text{g}/\text{m}^3$ with
401 higher concentrations observed during the summer months especially during July and August. A
402 unique source for this high summer concentration has not been identified. However, the increased
403 photochemical activities during the summer as compared to the winter months and the changes in
404 the emission of DMS due to higher biological activities in the ocean could possibly influence the
405 measured nss-sulfate concentration.

406 Elsewhere, seasonal trends have been observed for methanesulfonic acid (MSA) and DMS
407 which are known precursors of nss-sulfate with higher concentrations observed in the summer as
408 in the winter (Sciare et al. 2009). It has also been reported (Kouvarakis and Mihalopoulos 2002;
409 Kettle et al. 1999) that sea surface water temperature influences the production of nss-sulfate and
410 other organic materials in the ocean surface micro layer leading to pronounced seasonal cycle in
411 nss-sulfate concentrations with maximum observed in summer and minimum in winter. Studies in
412 the Mediterranean sea (a region with relatively high anthropogenic pollution) have evaluated the
413 biogenic contribution to nss-sulfate concentration to be between 6 % and 22 % (Ganor et al.
414 2000, Mihalopoulos et al. 1997). It has also been observed that under marine air mass conditions
415 the contribution of biogenic sources to nss-sulfate may rise up to 100 % (Bates et al. 1992). At
416 the CVAO, the minimum concentration of nss-sulfate during the winter and the summer was
417 about $0.20 \mu\text{g}/\text{m}^3$ and $0.70 \mu\text{g}/\text{m}^3$, respectively. As a first approximation, assuming that these
418 lowest concentrations of nss-sulfate were of biogenic contribution from the ocean, it would imply
419 that the biogenic contribution to the total nss-sulfate could be estimated to be averagely about 40
420 $\pm 20 \%$ in this region. Thus, although anthropogenic activities influence nss-sulfate
421 concentrations especially during the dust storm and in air masses coming from Europe via the
422 Moroccan coast, photochemical production of nss-sulfate and emission of marine precursors
423 could also have been important during the summer in this region.

424

425 **3.3.4 OM and EC**

426 These two carbon sum parameters showed a good correlation in their time series. The 5 year
427 average for OM and EC was $1.02 \pm 1.04 \mu\text{g}/\text{m}^3$ and $0.13 \pm 0.16 \mu\text{g}/\text{m}^3$, respectively. The
428 observed EC value was quite similar to the annual mean of $0.18 \mu\text{g}/\text{m}^3$ found by Nunes et al.
429 (2013) for the year 2011 on the island of Santiago which is a slightly more anthropogenically
430 influenced region than the CVAO. Figure 3 shows the variability in both EC and OM

431 concentration over the investigated time period. Elevated EC concentrations were strongly
432 connected to elevated OM concentration but not vice versa. The number of samples with elevated
433 OM concentration was greater than those with elevated EC concentration because of additional
434 natural single sources of OM, especially during the summer. High concentrations of OM and EC
435 were strongly correlated to air masses originating from the African continent.

436 During the Harmattan season (end of November to middle of March) aerosols from the African
437 continent carried not only Saharan dust but also anthropogenic emissions from ship tracks near
438 the African coast, the African coastal cities of Dakar, Nouakchott and sometimes biomass
439 burning aerosols (EC and OM) as well as biological material into the Cape Verde region (Milton
440 et al. 2008). During such periods the EC concentration was three times higher than in air masses
441 coming from Europe and five times higher than in marine air masses. The lower transport height
442 is a further important factor for the measured elevated concentrations of dust and other aerosol
443 components during the winter season. The averaged concentration of EC and OM given in Table
444 2 were in the same range as those recently reported for marine environments by Alves et al.
445 (2007). The lowest concentration for EC was found in dominant marine air masses.

446 It has been reported that biogenic material containing organic substances of low solubility in the
447 upper sea water layer are emitted via the surface micro layer (SML) into the atmosphere and are
448 found mainly in submicron particles (O'Dowd and De Leeuw 2007; Facchini et al. 2008; Müller
449 et al., 2009). Secondary organic aerosols formation from marine sources has also been reported in
450 different marine environment (Kawamura and Gagosian 1987; O'Dowd et al. 2004; Facchini et
451 al. 2010). In Figure 4, the monthly and interannual variation of OM and EC are presented. A
452 strong seasonal trend is observed for OM and EC with higher values observed during the winter
453 seasons as otherwise. This winter maximum is similar to that observed for the mass concentration
454 and it is attributed to the influence of continental air masses from Africa which often carries a lot
455 of Saharan dust as well as anthropogenically emitted particles. Beside the anthropogenic sources
456 of OM and EC, OM was also be emitted from the SML of the ocean itself. The amount of the
457 marine OM production depends on oceanic biological activity which has a distinct seasonality
458 (Sciare et al. 2009). A smaller summer maximum of OM (Figure 4) was also observed which had
459 its origin from direct marine emissions or in marine emissions of gaseous precursors of PM such
460 as dimethylsulphide (DMS), isoprene, organic amines and others (Gantt & Meshkidze, 2013).
461 The lowest OM concentrations were observed in April and October at CVAO. With the exception
462 of the high values observed for EC in May 2007 which was due to a dust storm during this

463 month, the EC values remain low throughout the other seasons. Thus, the high EC concentration
464 in this region was mostly due to long range transport from Africa in the dust season.

465

466 **3.3.5 Nitrogen containing ions**

467 Ammonium and nitrate showed no correlation amongst each other. These ions might have had
468 other sources. The 5-year average of ammonium and nitrate were 0.09 ± 0.1 and $1.1 \pm 0.1 \mu\text{g}/\text{m}^3$,
469 respectively. Clarke and Porter (1993) and Quinn et al. (1988) found similar ammonium
470 concentration in remote oceanic regions and suggested it could be of marine biogenic origin. The
471 concentration of both ions (ammonium and nitrate) was not influenced by the sampling height
472 implying their content in sea salt is very low. Nitrate like ammonium also showed strong
473 temporal variation (Figure 3). Ammonium concentrations varied from below detection limit to
474 $0.76 \mu\text{g}/\text{m}^3$ while nitrate concentrations varied from $0.14 \mu\text{g}/\text{m}^3$ to $3.7 \mu\text{g}/\text{m}^3$ (Table 2). This
475 strong variation was attributed to the changing air mass origin. In marine air masses the nitrate
476 concentration was lower than in air masses coming from the African or European continent
477 implying long range transport was a significant source of the observed nitrate concentrations. For
478 ammonium, summer concentrations were found to be 44 % higher than the winter concentrations
479 for clean marine air masses which would suggest that marine biological and photochemical
480 processes could strongly influence the ammonium concentrations in this region.

481 Nitrate concentrations, however, never showed a strong seasonal trend as shown on Figure 4. A
482 slight increase in the nitrate concentrations (about 20%) was often observed in the summer except
483 during 2008 where a strong decline in nitrate concentrations from January to December was
484 observed. Ammonium on the other hand, showed seasonal trends with annual maximum observed
485 in spring and early summer (Figure 4). As can be observed in Figure 4, ammonium seasonality
486 was not correlated with either the aerosol mass loading or the nss-sulfate trend. This suggests that
487 the observed ammonium in this region is not strongly linked to ammonium sulfate and may have
488 another major source different from long range transport from the continent. Marine sources of
489 NH_3 were reported earlier by Jickells et al. (2003) from isotopic measurements. Quinn et al.
490 (1988) also observed simultaneously high concentrations of ammonia in the Pacific Ocean and in
491 the oceans atmosphere and indicated that the ocean was the potential source of the ammonia.
492 They observed an averaged ammonium concentration of about $108 \text{ ng}/\text{m}^3$ in the remote north-east
493 Pacific Ocean in May which is within the same order of magnitude as that observed at CVAO
494 during May at $165 \pm 129 \text{ ng}/\text{m}^3$. Clarke and Porter (1993) have also shown good correlation

495 between atmospheric ammonium and chlorophyll A concentrations. Although long range
496 transport cannot be neglected, our results indicate that the ocean has a significant contribution to
497 the observed ammonium especially during the spring in this region.

498

499 **3.3.6 Calcium**

500 Calcium showed strong temporal variation throughout the year depending on the air mass origin
501 and sampling height (Figure 3). This variation indicates that calcium was both from sea spray and
502 mineral dust corresponding to, sea salt (ss) and nss-calcium. The calcium peaks were correlated
503 with either peaks in aerosol mass loading or sea salt concentrations. The minimum and maximum
504 concentrations were $0.01 \mu\text{g}/\text{m}^3$ and $4.44 \mu\text{g}/\text{m}^3$, respectively. The maximum and minimum
505 values were related to days of Saharan dust events and days of dominant marine air mass inflow,
506 respectively. A strong correlation between nss-calcium and total soluble calcium (with $r^2 = 0.98$)
507 during dust events confirmed that the Saharan dust was the main source of nss-calcium in these
508 samples. Thus, soluble nss-calcium was often a good indicator for Saharan dust in this region.
509 Calcium-rich aerosol was often mobilized from NW-Sahara. During the atmospheric transport the
510 unsoluble CaCO_3 was processed to more soluble compounds, e.g. in clouds. Sea salt and mineral
511 dust contributed $0.15 \pm 0.15 \mu\text{g}/\text{m}^3$ and $0.49 \pm 0.48 \mu\text{g}/\text{m}^3$, respectively, to the total soluble
512 calcium average concentration of $0.64 \pm 0.63 \mu\text{g}/\text{m}^3$.

513

514 **3.3.7 Potassium and Magnesium**

515 Variations in potassium and magnesium concentrations were also attributed to the varying air
516 mass inflow and the different sampling height with maximum concentrations of potassium and
517 magnesium observed at $0.86 \mu\text{g}/\text{m}^3$ and $1.34 \mu\text{g}/\text{m}^3$, respectively (Table 2). The 5 year average
518 concentration at the tower of potassium and magnesium were $0.13 \pm 0.09 \mu\text{g}/\text{m}^3$ and $0.40 \pm$
519 $0.20 \mu\text{g}/\text{m}^3$, respectively, of which nss-potassium and nss-magnesium made up only 0.02 ± 0.06
520 $\mu\text{g}/\text{m}^3$ and $0.02 \pm 0.04 \mu\text{g}/\text{m}^3$ of the total average, respectively. This corresponds to only about 10
521 % of potassium and 5% of magnesium. Thus the ocean was the main source of these ions in this
522 region. Nss-potassium peaks were often linked with nss-calcium and mass loading peaks,
523 implying continental air masses from Africa could account for some of the nss-potassium
524 concentrations found in this region.

525 **3.3.8 Oxalate**

526 Oxalate concentrations were low in comparison to those reported in urban and continental

527 aerosols. Table 4 shows an overview of the measured oxalate concentration and those of other
528 reported works. The average oxalate concentration during polluted air masses was about $0.12 \pm$
529 $0.06 \mu\text{g}/\text{m}^3$. This value was twice as much as the concentrations observed during marine air mass
530 inflow. Comparatively to reported oxalate concentrations (Table 4), the observed concentrations
531 were within reported range. The values were higher than those reported in other marine
532 environments such as in Mace Head or Amsterdam Island (Rinaldi et al. 2011) but lower than
533 those reported in continental aerosols such as in Hong Kong (Yao et al. 2002) or Sapporo, Japan
534 (Pavuluri et al. 2012). The differences between the results in this study and the above mentioned
535 works is strongly related to the different air mass inflow regions in these areas. Mace Head is
536 more remote than CVAO while Hong Kong and Sapporo are more urban than CVAO.

537 In general, elevated oxalate concentrations were observed in polluted European and African air
538 masses (Table 4). The maximum oxalate concentration was measured at $0.46 \mu\text{g}/\text{m}^3$ in September
539 2009 during a period where air mass originated from West Africa. During the Saharan dust
540 influenced winter days, the oxalate concentration was higher than during non-dust winter days.
541 The high values were usually connected to dust storms while peaks in oxalate concentrations
542 during the summer season were connected to periods of high photochemical activity, high marine
543 activities whereby potential oxalate precursors could have been emitted to the atmosphere and
544 periods when other precursors that might have been transported from Europe. A distinct
545 seasonality in oxalate concentration was observed with a maximum during the summer season
546 (June to August). The formation of oxalate depends on the presence of organic precursors, such
547 as ethene (Warneck 2003), glyoxal (Carlton et al. 2007), and sunlight which are more available
548 during the summer.

549

550 *Please insert Table 4 here*

551

552 In general, the aerosol chemical composition was influenced by sea-salt, organic compounds
553 emitted from the ocean surface micro layer, organic matter, and long range transported particulate
554 matter or precursors from anthropogenic emissions in northwestern Africa, the Canary Islands,
555 and the European continent. The Cape Verde islands themselves were only a minor source of PM
556 because of the prevailing North-East trade winds and the location of the CVAO at the
557 northeastern shore of the island São Vicente.

559 **3.4 Inter-relationship between ionic species**

560 **3.4.1 Nitrate and nss-sulfate**

561 Nitrate and nss-sulfate showed good correlations during the winter and the summer ($r^2 = 0.72$)
562 seasons (Nov-Apr and May-Oct, Figure 5) which could be attributed to their anthropogenic origin
563 due to observation of frequent elevation of these concentrations during long range transport from
564 Europe and Africa.

565

566 *Please insert Figure 5 here*

567

568 The higher slope of the regression line during summer in comparison to that of winter is
569 indicative of the presence of an additional source of nss-sulfate such as the production through
570 photochemical processes. In principle, both ions in the particle phase or their gas phase
571 precursors might be transported in higher amounts from the European and African continent
572 during winter.

573 However, during summer the photochemical production of particle phase nitrate and sulfate is
574 higher. This may therefore lead to the observed increase in the nss-sulfate concentration reflected
575 by the increase in the slope. The combined effects of increased winter emissions of anthropogenic
576 precursors reduced winter and enhanced summer photochemical conversion might explain the
577 effect depicted in Figure 5. However, further investigations are necessary in order to clearly
578 explain the depicted difference.

579

580 **3.4.2 Nss-sulfate and Oxalate**

581 The scatter plot of nss-sulfate and oxalate shows weak correlation between both species during
582 winter and summer. However, the winter correlation (Fig. 6a) was weaker than the summer
583 correlation with a lot of scattering in the data. These correlations were only observed during days
584 with high marine air mass influence and low aerosol mass loading with negligible influence from
585 anthropogenic emissions. During a period of eleven days with dominant marine influenced air
586 mass in spring 2011, an even stronger correlation between nss-sulfate and oxalate ($r^2 = 0.90$) was
587 observed (Fig. 6c). This suggests that there is a strong influence of surface water temperatures on
588 oxalate and nss-sulfate concentrations. It can be assumed that the clean air mass was fed only by
589 marine emissions of DMS, ethene and other marine organic precursors and subsequent

590 photochemical aqueous phase reactions might have led to the formation of oxalate (Tilgner and
591 Herrmann 2010). As mentioned above, high surface water temperature are known to also
592 influence the production of nss-sulfate. Thus we conclude that both nss-sulfate and oxalate
593 within this period could have originated from different precursors of marine origin such as from
594 marine organisms' e.g algae or from their emissions.

595

596 *Please insert Figure 6 here*

597

598 **3.4.3 Ammonium and chlorophyll A**

599 Figure 7 shows the concentration profiles of ammonium, chlorophyll A and oxalate. The
600 temporal variability of ammonium and chlorophyll A showed similar trends implying a
601 coincidence of these species. Increase in ammonium concentration was often correlated with an
602 increase in chlorophyll A concentration in the ocean's surface. The chlorophyll A concentration
603 was taken from monthly averaged MODIS Aqua satellite images over a region east and northeast
604 of São Vicente achieved from <http://disc.sci.gsfc.nasa.gov/giovanni/overview/index.html>. The
605 chlorophyll A maximum was observed between May and June. Chlorophyll A concentrations in
606 the region northeast of Cape Verde is usually higher in spring than in the other seasons and it is
607 influenced by the delivery of nutrients by higher upwelling intensity (Lathuiliere et al. 2008;
608 Ohde and Siegel 2010) in the Mauritanian upwelling region. The observed coincidence between
609 ammonium and chlorophyll A suggest that the ocean might be a source of ammonium in this
610 region as previously explained above.

611

612 *Please insert Figure 7 here*

613

614 A similar correlation between chlorophyll A and ammonium has been reported before. Clarke
615 and Porter (1993) found good correlation between enhanced ammonium aerosol concentrations
616 and enhanced chlorophyll concentrations during an equatorial Pacific Ocean cruise and
617 concluded the observed ammonia was a result of equatorial upwelling. Jickells et. al. (2003) also
618 concluded on the basis of isotopic measurements of ammonium in marine aerosols that the ocean
619 was a possible source of their observed ammonium concentrations in the North and South
620 Atlantic Ocean.

621 Quinn et al. 1988 also observed ammonia in the remote Pacific Ocean and the atmosphere and

622 concluded that the observed atmospheric ammonium originated from the ocean. Although the
623 ocean is a significant source of ammonia during remote conditions, long range transport of
624 ammonia or ammonium salts from the African continent or SW Europe were also important
625 sources of ammonia in this region.

626

627 **3.4.4 Elemental carbon (EC) and nss-potassium**

628 A similar temporal variation was observed in the time series of nss-potassium and elemental
629 carbon concentrations during dust events when elevated OC and EC concentrations were
630 observed (Figure 8) with correlation factor ($r^2 = 0.6$). In principle, this correlation was only
631 observed during about 50% of the time when air mass inflow was from Africa. Nss-potassium is
632 a known tracer for biomass burning activities. This correlation thereby suggests that biomass
633 burning could partly account for the observed EC concentrations at CVAO especially during air
634 mass inflow from Africa. However, when the air mass origin was from Europe or from the
635 oceans, no correlation could be observed between nss-potassium and EC.

636

637 *Please insert Figure 8 here*

638

639 **3.5 Bromide and chloride depletion in PM₁₀**

640 Bromide and chloride deficits indicate significant reactive cycling of halogens and do influence
641 the reactive capacity of the marine environment by the release of more reactive chloride to the
642 atmosphere. Bromide and chloride deficits in marine aerosols have been reported in different
643 marine environments (Kerminen et al. 1998; Yao and Zhang 2012; Mozurkewich 1995, Kumar
644 A, and Sarin M., 2010). The reported (Liebezeit 2011) sodium to chloride (bromide) mass ratio in
645 sea-salt is 0.56 (162.4), and the molar ratio is 0.85 (46.73). The chloride (bromide) depletion is
646 estimated as the percentage loss in chloride (bromide) from sea salt chloride (bromide)
647 concentrations leading to higher values of the sodium to chloride (bromide) ratios. In the
648 atmosphere, when bromide and chloride react with acidic gases or particles containing nitric,
649 sulfuric, or organic acids to form HOX, X₂ and other compounds, the evaporation of volatile
650 bromine/chlorine compounds occur and bromide and chloride losses are observed in marine
651 aerosols leading to an increase in the sodium to chloride (bromide) ratio. This effect of
652 bromide/chloride depletion is known to increase with decreasing particle size from about 30 % to

653 100 % in the presence of anthropogenic pollutants (Hsu et al. 2007; Quinn and Bates 2005). In
654 this study, bromide and chloride depletion was observed in PM₁₀ samples and are discussed
655 according to seasons, sampling height and dust concentration.

656

657 *Please insert Figure 9 here*

658 *Please insert Table 5 here*

659

660 Figure 9 shows the temporal variation in the chloride/bromide depletion and aerosol mass
661 concentration during 5 years of measurements at CVAO. Bromide loss was always higher than
662 chloride loss with average bromide and chloride losses of about 80 % and 16 %, respectively.
663 Periods of Saharan dust influence observed as peaks in the aerosol mass concentrations, usually
664 yielded low bromide (62 %)/chloride (9 %) loss as otherwise. The lowest depletions were
665 observed when measurements were performed close to the coastline at a 4 m sampling height.

666 At lower sampling height, fresh sea spray particles have shorter residence time in the atmosphere
667 prior to their collection and thus should have insignificant bromide/chloride deficits. However,
668 due to the mixture of aged and long range transported aerosols with the freshly emitted marine
669 particles, bromide (chloride) depletions of about 4 % was observed at this height. In Table 5 the
670 average chloride and bromide deficits for the typical air mass inflow of the particles and their
671 precursors are given. Higher halogen depletion was observed during periods of low aerosol mass
672 concentration with less influence of Saharan dust. Long range transported and aged sea-salt
673 particles loose more chloride (bromide) due to their long atmospheric residence time and thus
674 more time for interaction with acidic compounds. The highest chloride (bromide) loss of about
675 30% (87 %) was observed when air mass crossed southwest Europe prior to its arrival at CVAO
676 and had relatively long (72 h) residence time over the ocean. The more anthropogenically
677 influenced SW European particles and gaseous compounds thus had sufficient time to adsorb
678 onto andreact with sea salt particles resulting in a higher exchange and displacement of
679 halogenides from sea salt particles as compared to periods when particles spends less time over
680 the ocean as it's the case during Saharan dust events.

681 The chloride depletion during winter and summer marine air masses (Figure 1A), was about 5%
682 lower than the loss observed during SW Europe influenced air mass inflow. The air mass origin,
683 aerosol acidic component concentration and the sea salt particle atmospheric life time were the
684 determining factors towards the halogenide depletion. The deficits were higher in the summer

685 than in the winter. This was likely due to varying solar irradiation intensity and the concentration
686 difference of the aerosol acidic components of sulfuric and nitric acid in these samples. During
687 marine influenced air mass inflow the nss-sulfate concentration in the summer was twice as much
688 as that observed in the winter, likely due to the increase in photochemical production activities
689 and the emission of marine nss-sulfate precursors as previously explained. Thus the additional
690 nss-sulfate source and higher solar irradiation are most probably one of the reasons for the
691 increased chloride/bromide loss during the summer in comparison to the winter for marine
692 influenced air masses.

693 Nevertheless, although the concentration of nitrate and non-sea salt sulfate was high during
694 Saharan dust events, the chloride/bromide depletion was found to be the lowest. Figure 9 depicts
695 a clear anti-correlation between PM mass concentration and halogenide loss. This effect was
696 clearly seen in winter 2007/08 and 2010/11. During the winter 2008/09 the dust events were less
697 intensive and the winter sampling period 2009/10 took place at a lower sampling height with a
698 greater influence of sea spray.

699 During dust events, there is not only an increase in acidic species, but also an increase in cations
700 and carbonates. The increase in cations concentration provides additional reactive sites for the
701 acidic species thus reducing the possibility for the direct reaction on sea salt particles, and
702 therefore, decreasing the overall displacement of halogenides from sodium. Furthermore, gaseous
703 halogenides could react with CaCO_3 as shown by Sullivan et al. (2007) leading to a buffering
704 effect of the dust on the sea salt particles, thereby resulting in a more externally mixed aerosol.
705 Thus a combination of low residence time as mentioned above and higher competition of cations
706 sites during dust events leads to a lower effective loss of chloride and bromide from sea salt
707 particles in comparison to the other situations. We thus suggest that in this region of the Atlantic,
708 these three processes, photochemistry, air mass residence time and concentration of acidic
709 components are the determining driving factors towards halogenide deficits in the observed
710 aerosol.

711

712 **3.5.1 Contribution of acidic species to chloride depletion**

713 The most important aerosol acidic species are nitric and sulfuric acids since their concentrations
714 are far higher than those of other acidic species such as oxalic acid (in non-dusty aerosol). As
715 explained above, the highest chloride deficit was observed when air mass inflow was from
716 Europe. The scatter plot of equivalent concentrations of Na^+ and Cl^- (Figure 10a) shows that the

717 data points fall below the theoretical values in sea water and only approaches this line when the
718 Cl^- concentration is matched with nitrate and nss-sulfate concentrations (Figure 10b). Thus,
719 assuming all available nitrate and nss-sulfate species were involved in chloride depletion, this
720 would account only for about 90% of the chloride depletion. The actual contribution of these
721 species is, however, much less since they may also be associated with NH_4^+ , nss- K^+ or Ca^{2+} that
722 are possible neutralizers of the available nitric and sulfuric acids. Thus, considering the
723 neutralization of sulfuric or nitric acid by ammonium or other cations, the excess sulfuric or nitric
724 acid available will be even less and they would thus account for less than 90% of the chloride
725 depletion. This indicates that during air mass inflow from Europe other process mechanisms
726 different from acid displacement reactions such as photochemical reactions with ozone or NO
727 (Behnke and Zetzsch 1990) could have been involved in chloride depletion.

728

729 *Please insert Figure 10 here*

730

731 A similar tendency was observed in samples where air mass inflow was of marine origin during
732 the summer. The estimated chloride loss was about 26 % and the concentrations of the acidic
733 components were also elevated, but the acid displacement of neither nitric nor sulfuric acids was
734 sufficient to account for the chloride loss. Their contribution however could only explain about
735 95 % of the chloride loss assuming these species were not associated with other cations. The only
736 situation whereby acidic species could sufficiently account for chloride loss was during Saharan
737 dust events as shown in Figure 9c and 9d. The scatter plot shows good correlation slightly above
738 theoretical sea water line for Na^+ and Cl^- when Cl^- concentrations are matched with NO_3^- ,
739 indicating that, within error margins, nitric acid displacement was the main reaction leading to
740 chloride loss during dust events. This claim is supported by results of size resolved distribution of
741 aerosol components previously reported by Müller et al. (2010) which showed that during dust
742 events, about 90 % of nitrate is found in the coarse mode together with sea salt particles while
743 nss-sulfate concentration are concentrated in the fine mode. Thus in all non-Saharan dust
744 influenced days at CVAO, photochemistry was a determining factor towards chloride loss, while
745 during dust events, nitric acid played the major role.

746

747

748 **3.6 PMF source apportionment analysis**

749 The positive matrix factorization analysis (PMF) was applied to identify the possible sources of
750 the aerosol observed at the CVAO during the investigated time period. The chemical composition
751 matrix was made of the 12 analyzed chemical species (water soluble ions, OC and EC). Three
752 major sources were identified by having clear different signatures as fresh sea-salt, aged sea-salt
753 and long range transport. Figure 11 shows the source profiles (blue bars) and the relative
754 contribution of each factor to the total species concentration in the samples (red squares). There
755 was no ideal tracer for mineral dust since trace metal analysis were not performed on these filters.
756 However, due to the strong correlation between nss-Ca²⁺ and Ca²⁺ during dust storms ($r^2 = 0.99$),
757 calcium occurrence was considered as a possible indicator of mineral dust or long range
758 transported dust particles. The fresh sea salt factor was characterized by similar (Liebezeit 2011)
759 sea water proportions of Na (35 %), Cl (54 %), sulfate (7 %) and magnesium (4 %). The model
760 obtained fractions were quite similar to reported sea water concentration and indicated that PMF
761 is a useful tool in identifying sources in complex aerosol samples. In principle, this factor
762 represents freshly emitted sea salt particles due the strong agreement with sea water proportions
763 and the little association with non-sea salt species. Thus, freshly emitted sea salt particles
764 dominated the ionic composition of the aerosol as it made up about 50 % of its ionic and organic
765 matter content (Figure 12). This factor could account for the total bromide and 50 % of chloride,
766 sodium, potassium and magnesium concentrations in the samples.

767

768 *Please insert Figure 11 and Figure 12 here*

769

770 The aged sea salt source was the second most important source making up about 36% of the total
771 ionic and organic mass. It was characterized by elevated sulfate (14 %), nitrate (6 %) and OC
772 (4 %) concentrations associated with sea salt particles. This source describes sea salt particles that
773 interact with acidic gases or marine emitted organic matter such as SOA and nss-sulfate from
774 DMS chemistry. The lower chloride (42 %) to sodium (31 %) ratio in this factor is a strong
775 indication of chloride loss due to one of the processes mentioned above. As has also been
776 reported in other works (Amato et al. 2009), sulfate and nitrate association with sea salt particles
777 in this work was also considered as an indicator for the aged sea salt source. This source could
778 account for about 62 % of the total observed soluble calcium, 58 % of the sulfate, 45 % of the

779 nitrate and 25 % of the organic matter observed in the samples.

780 Finally, the long range transport factor was characterized by calcium, organic and elemental
781 carbon, as well as elevated sulfate and nitrate concentrations. This factor could explain 14% of
782 the source of the investigated ionic and organic components. The unique tracer for this factor was
783 the presence of EC. EC as well as OC can originate from traffic emissions, biomass burning, or
784 ship emissions. Emitted particles from such anthropogenic activities may only reach the CVAO
785 via long range transport. This factor could account for the presence of all EC, 80% of the OC and
786 60% of the nitrate observed at the CVAO. A comparison of this factor with our Saharan dust
787 estimation showed most of the time a similar time series. Therefore, the estimated mineral dust
788 profile could be explained by the long range transport source.

789 Although the PMF model could not successfully separate mineral dust and long range transported
790 particles due to the limited data input, the obtained results are still representative of this region of
791 the Atlantic and are unique and show that mineral dust contributes to not more than 14 % of the
792 water soluble ions and organic mass budget at CVAO.

793

794 **4. Conclusions**

795 Saharan dust and sea salt dominate the PM_{10} aerosol constitution in near surface air masses at the
796 CVAO. At the standard collection height of 32 m at the CVAO, the long term mean of sea salt
797 and total PM_{10} aerosol were $11 \mu g/m^3$ and $47 \mu g/m^3$, respectively, of which Saharan dust made up
798 55% of the PM_{10} mass. Secondary ionic species, elemental carbon, organic matter and water
799 completed the particle constitution. Seasonal variations were found for aerosol mass, dust, nss-
800 sulfate, EC, OM and ammonium.. Ammonium and oxalate were often correlated with chlorophyll
801 A which suggests that ammonia and oxalic acid had also marine precursors in this environment.
802 A distinct seasonality was observed for the halogenide depletion with the minimum in winter due
803 to the occurrence of Saharan dust events and the lower irradiation intensity in non-dust periods.
804 Chloride depletion varied between 10 % and 35 %. In marine air masses during the summer and
805 in polluted air masses from SW Europe, bromide was often fully depleted while chloride
806 observed its highest depletions. Photochemistry, air mass residence time and concentration of
807 acidic components were the main factors controlling halogenide depletion in this region. While
808 photochemistry was decisive during summer, nitric acid played a major role towards chloride
809 depletion during dust storms.

810 Ground based long-term investigation of PM at the CVAO is an important step towards
811 understanding the role of aerosols in ocean atmosphere interactions especially in the tropical
812 Northeast Atlantic. The observed strong annual and seasonal variation of the aerosol constitution
813 provides useful information to the type of atmospheric nutrient deposition and the ocean responds
814 to this deposition over the past five years. Such investigations are quite useful since they provide
815 the relevant background knowledge for understanding in the long term the role the atmosphere
816 and the Ocean plays in the global climate. Such long term observations are highly encouraged
817 and would be essential in initializing model runs that can then in more detail describe the link
818 between the atmosphere ocean interaction and the global climate. Air mass origins with dust
819 source regions, oceanic and meteorological influences during air mass transport must be further
820 investigated to understand their effects on the global climate.

821

822 **Acknowledgements**

823 The efforts of Luis Mendes and Helder Timas Nascimento for sampling and maintenance
824 activities at the CVAO and of the TROPOS laboratory assistants for their helpful work are
825 greatly appreciated. The study was supported by the German BMBF within the SOPRAN I and II
826 projects (FKZ: 03F0462J and 03F0611J) and the EU specific Support Action TENATSO
827 (37090).

828

829

830

831

832

833

834

835

836

837

838

839

840

841

842 **5.0 References**

843 Alastuey, A., Querol, X., Castillo, S., Escudero, M., Avila, A., Cuevas, E., Torres, C., Romero, P.M., Exposito, F., Garcia, O., Diaz, J.P., Van Dingenen, R., Putaud, J.P.: Characterisation of TSP and PM_{2.5} at Izana and Sta. Cruz de Tenerife (Canary Islands, Spain) during a Saharan Dust Episode (July 2002). *Atmos. Environ.* 39(26), 4715-4728, 2005.

847 Allan, J.D., Topping, D.O., Good, N., Irwin, M., Flynn, M., Williams, P.I., Coe, H., Baker, A.R.,
848 Martino, M., Niedermeier, N., Wiedensohler, A., Lehmann, S., Muller, K., Herrmann, H.,
849 McFiggans, G.: Composition and properties of atmospheric particles in the eastern Atlantic and
850 impacts on gas phase uptake rates. *Atmos. Chem. Phys.* 9(23), 9299-9314, 2009.

851 Alves, C., Oliveira, T., Pio, C., Silvestre, A.J.D., Fialho, P., Barata, F., Legrand, M.:
852 Characterisation of carbonaceous aerosols from the Azorean Island of Terceira. *Atmos. Environ.*
853 41(7), 1359-1373, 2007.

854 Amato, F., Pandolfi, M., Escrig, A., Querol, X., Alastuey, A., Pey, J., Perez, N., Hopke, P.K.,
855 Quantifying road dust resuspension in urban environment by Multilinear Engine: A comparison
856 with PMF2. *Atmospheric Environment* 43, 2770-2780, 2009.

857 Anguelova, M. D, Whitecaps, sea-salt aerosols, and climate, Ph.D. Dissertation, University of
858 Delaware, 2002.

859 Bates, T.S., Lamb, B.K., Guenther, A., Dignon, J., Stoiber, R.E.: Sulfur Emissions to the
860 Atmosphere from Natural Sources. *J. Atmos. Chem.* 14(1-4), 315-337, 1992.

861 Bates, T.S., Quinn, P.K., Coffman, D.J., Johnson, J.E., Miller, T.L., Covert, D.S., Wiedensohler,
862 A., Leinert, S., Nowak, A., Neususs, C.: Regional physical and chemical properties of the marine
863 boundary layer aerosol across the Atlantic during Aerosols99: An overview. *J. Geophys. Res.-*
864 *Atmos.* 106(D18), 20767-20782, 2001.

865 Behnke, W. and C. Zetzsch. 1990. Heterogeneous Photochemical Formation of Cl-Atoms from
866 NaCl Aerosol, NO_x and Ozone. *Journal of Aerosol Science* 21:S229-S232.

867

868 Canonaco, F., Crippa, M., Slowik, J. G., Prévôt, A. S. H., and Baltensperger, U.: SoFi, an Igor
869 based interface for the efficient use of the generalized multilinear engine (ME-2) for source
870 apportionment: application to aerosol mass spectrometer data, *Atmos. Meas. Tech. Discuss.*, 6,
871 6409 - 6443, 2013.

872 Carlton, A.G., Turpin, B.J., Altieri, K.E., Seitzinger, S., Reff, A., Lim, H.J., Ervens, B.: Atmospheric
873 oxalic acid and SOA production from glyoxal: Results of aqueous photooxidation
874 experiments. *Atmos. Environ.* 41(35), 7588-7602, 2007.

875 Carpenter, E.J., Subramaniam, A., Capone, D.G.: Biomass and primary productivity of the
876 cyanobacterium *Trichodesmium* spp. in the tropical N Atlantic ocean. *Deep-Sea Res. Pt. I* 51(2),
877 173-203, 2004.

878 Carpenter, L.J., Fleming, Z.L., Read, K.A., Lee, J.D., Moller, S.J., Hopkins, J.R., Purvis, R.M.,
879 Lewis, A.C., Müller, K., Heinold, B., Herrmann, H., Fomba, K.W., van Pinxteren, D., Muller, C.,
880 Tegen, I., Wiedensohler, A., Müller, T., Niedermeier, N., Achterberg, E.P., Patey, M.D.,
881 Kozlova, E.A., Heimann, M., Heard, D.E., Plane, J.M.C., Mahajan, A., Oetjen, H., Ingham, T.,
882 Stone, D., Whalley, L.K., Evans, M.J., Pilling, M.J., Leigh, R.J., Monks, P.S., Karunaharan, A.,
883 Vaughan, S., Arnold, S.R., Tschritter, J., Pohler, D., Friess, U., Holla, R., Mendes, L.M., Lopez,
884 H., Faria, B., Manning, A.J., Wallace, D.W.R.: Seasonal characteristics of tropical marine
885 boundary layer air measured at the Cape Verde Atmospheric Observatory. *J. Atmos. Chem.* 67(2-
886 3), 87-140, 2010.

887 Chen, Y. and Siefert, R.L.: Determination of various types of labile atmospheric iron over remote
888 oceans. *J. Geophys. Res. -Atmos.* 108(D24), 2003.

889 Chen, Y. and Siefert, R.L.: Seasonal and spatial distributions and dry deposition fluxes of
890 atmospheric total and labile iron over the tropical and subtropical North Atlantic Ocean.
891 *J. Geophys. Res.-Atmos.* 109(D9), 2004.

892 Chiapello, I., Bergametti, G., Gomes, L., Chatenet, B., Dulac, F., Pimenta, J., Suares, E.S.: An
893 Additional Low Layer Transport of Sahelian and Saharan Dust over the North-Eastern Tropical
894 Atlantic. *Geophys. Res.Lett.* 22(23), 3191-3194, 1995.

895 Chiapello, I., Prospero, J.M., Herman, J.R., Hsu, N.C.: Detection of mineral dust over the North
896 Atlantic Ocean and Africa with the Nimbus 7 TOMS. *J. Geophys. Res.-Atmos.* 104(D8), 9277-
897 9291, 1999.

898 Clarke, A.D., Porter, J.N.: Pacific Marine Aerosol .2. Equatorial Gradients in Chlorophyll,
899 Ammonium, and Excess Sulfate during Saga-3. *J. Geophys. Res.-Atmos.* 98(D9), 16997-17010,
900 1993.

901 Cropp, R.A., Gabric, A.J., McTainsh, G.H., Braddock, R.D., Tindale, N.: Coupling between
902 ocean biota and atmospheric aerosols: Dust, dimethylsulphide, or artifact? *Global
903 Biogeochem.Cy.*19(4), 2005.

904 deLeeuw, G., Neele, F.P., Hill, M., Smith, M.H., Vignati, E.: Production of sea spray in the surf
905 zone. *J. Geophys. Res.-Atmos.* 105(D24), 29397-29409, 2000.

906 Facchini, M.C., Decesari, S., Rinaldi, M., Carbone, C., Finessi, E., Mircea, M., Fuzzi, S., Moretti,
907 F., Tagliavini, E., Ceburnis, D., O'Dowd, C.D.: Important Source of Marine Secondary Organic
908 Aerosol from Biogenic Amines. *Environ.Sci. Technol.* 42(24), 9116-9121, 2008.

909 Facchini, M.C., Decesari, S., Rinaldi, M., Finessi, E., Ceburnis, D., O'Dowd, C.D., Stephanou,
910 E.G.: Marine SOA: Gas-to-particle conversion and oxidation of primary organic aerosol.
911 *Geochim.Cosmochim. Ac.* 74(12), A275-A275, 2010.

912 Fomba, K. W., Müller, K., Herrmann, H.: Aerosol size-resolved trace metal composition in
913 remote northern tropical Atlantic marine environment: Case study Cape Verde Islands, *Atmos.
914 Chem. Phys.*, 13, 1-14, 2013.

915 Formenti, P., Elbert, W., Maenhaut, W., Haywood, J., Andreae, M.O.: Chemical composition of
916 mineral dust aerosol during the Saharan Dust Experiment (SHADE) airborne campaign in the
917 Cape Verde region, September 2000. *J.Geophys.Res.-Atmos.* 108(D18), 2003.

918 Formenti, P., Schutz, L., Balkanski, Y., Desboeufs, K., Ebert, M., Kandler, K., Petzold, A.,
919 Scheuvens, D., Weinbruch, S., Zhang, D.: Recent progress in understanding physical and
920 chemical properties of African and Asian mineral dust. *Atmos. Chem. Phys.* 11(16), 8231-8256,
921 2011.

922 Ganor, E., Foner, H.A., Bingemer, H.G., Udisti, R., Setter, I.: Biogenic sulphate generation in the
923 Mediterranean Sea and its contribution to the sulphate anomaly in the aerosol over Israel and the
924 Eastern Mediterranean. *Atmos. Environ.* 34(20), 3453-3462, 2000.

925 Gantt, B. and Meshkidze, N.: The physical and chemical characteristics of marine primary
926 organic aerosol: a review. *Atmos. Chem. Phys.*, 13, 3979-3996, 2013.

927 Gelado-Caballero, M.D., Lopez-Garcia, P., Prieto, S., Patey, M.D., Collado, C., Hernandez-Brito,
928 J.J.: Long-term aerosol measurements in Gran Canaria, Canary Islands: Particle concentration,
929 sources and elemental composition. *J.Geophys.Res.-Atmos.* 117, 2012.

930 Gnauk, T., Müller, K., van Pinxteren, D., He, L.Y., Niu, Y.W., Hu, M., Herrmann, H.: Size-
931 segregated particulate chemical composition in Xinken, Pearl River Delta, China: OC/EC and
932 organic compounds. *Atmos. Environ.* 42(25), 6296-6309, 2008.

933 Harrison, R.M., Jones, A.M., Lawrence, R.G.: A pragmatic mass closure model for airborne
934 particulate matter at urban background and roadside sites. *Atmos. Environ.* 37(35), 4927-4933,
935 2003.

936 Heller, M.I. and Croot, P.L.: Superoxide decay as a probe for speciation changes during dust
937 dissolution in Tropical Atlantic surface waters near Cape Verde. *Mar. Chem.* 126(1-4), 37-55,
938 2011.

939 Hsu, S.C., Liu, S.C., Kao, S.J., Jeng, W.L., Huang, Y.T., Tseng, C.M., Tsai, F., Tu, J.Y., Yang,
940 Y.: Water-soluble species in the marine aerosol from the northern South China Sea: High
941 chloride depletion related to air pollution. *J.Geophys.Res.-Atmos.* 112(D19), 2007.

942 Jaenicke, R.: Atmospheric Aerosols and Global Climate. *J. Aerosol. Sci.* 11(5-6), 577-588, 1980.

943 Jickells, T.D., Kelly, S.D., Baker, A.R., Biswas, K., Dennis, P.F., Spokes, L.J., Witt, M.,
944 Yeatman, S.G.: Isotopic evidence for a marine ammonia source. *Geophys. Res. Lett.* 30(7), 2003.

945 Johansen, A.M., Siefert, R.L., Hoffmann, M.R.: Chemical composition of aerosols collected over
946 the tropical North Atlantic Ocean. *J. Geophys. Res.-Atmos.* 105(D12), 15277-15312, 2000.

947 Kandler, K., Benker, N., Bundke, U., Cuevas, E., Ebert, M., Knippertz, P., Rodriguez, S., Schutz,
948 L., Weinbruch, S.: Chemical composition and complex refractive index of Saharan Mineral Dust
949 at Izana, Tenerife (Spain) derived by electron microscopy. *Atmos. Environ.* 41(37), 8058-8074, 2007.

950 Kandler, K., Lieke, K., Benker, N., Emmel, C., Kupper, M., Muller-Ebert, D., Ebert, M.,
951 Scheuvens, D., Schladitz, A., Schutz, L., Weinbruch, S.: Electron microscopy of particles
952 collected at Praia, Cape Verde, during the Saharan Mineral Dust Experiment: particle chemistry,
953 shape, mixing state and complex refractive index. *Tellus B* 63(4), 475-496, 2011.

954 Kawamura, K. and Gagosian, R.B.: Implications of Omega-Oxocarboxylic Acids in the Remote
955 Marine Atmosphere for Photooxidation of Unsaturated Fatty-Acids. *Nature* 325(6102), 330-332,
956 1987.

957 Kawamura, K., Sakaguchi, F.: Molecular distributions of water soluble dicarboxylic acids in
958 marine aerosols over the Pacific Ocean including tropics. *J.Geophys.Res.-Atmos.* 104(D3), 3501-
959 3509, 1999.

960 Kelly, J.T., Chuang, C.C., Wexler, A.S.: Influence of dust composition on cloud droplet
961 formation. *Atmos. Environ.* 41(14), 2904-2916, 2007.

962 Kerminen, V.M., Teinila, K., Hillamo, R., Pakkanen, T.: Substitution of chloride in sea-salt
963 particles by inorganic and organic anions. *J. Aerosol Sci.* 29(8), 929-942, 1998.

964 Kettle, A.J., Andreae, M.O., Amouroux, D., Andreae, T.W., Bates, T.S., Berresheim, H.,
965 Bingemer, H., Boniforti, R., Curran, M.A.J., DiTullio, G.R., Helas, G., Jones, G.B., Keller, M.D.,
966 Kiene, R.P., Leck, C., Levasseur, M., Malin, G., Maspero, M., Matrai, P., McTaggart, A.R.,
967 Mihalopoulos, N., Nguyen, B.C., Novo, A., Putaud, J.P., Rapsomanikis, S., Roberts, G.,
968 Schebeske, G., Sharma, S., Simo, R., Staubes, R., Turner, S., Uher, G.: A global database of sea
969 surface dimethylsulfide (DMS) measurements and a procedure to predict sea surface DMS as a
970 function of latitude, longitude, and month. *Global Biogeochem.Cy.* 13(2), 399-444, 1999.

971 Kouvarakis, G. and Mihalopoulos, N.: Seasonal variation of dimethylsulfide in the gas phase and
972 of methanesulfonate and non-sea-salt sulfate in the aerosols phase in the Eastern Mediterranean
973 atmosphere. *Atmos. Environ.* 36(6), 929-938, 2002.

974 Kumar, A. and Sarin, M.M., Atmospheric water soluble constituents in fine and coarse mode
975 aerosols from high altitude site in western India: Long-range transport and seasonal variability.
976 *Atmos. Environ.* 44, 1245-1254, 2010.

977 Lathuiliere, C., Echevin, V., Levy, M.: Seasonal and intraseasonal surface chlorophyll-a
978 variability along the northwest African coast. *J.Geophys.Res.-Oceans* 113(C5), 2008.

979 Lee, J.D., McFiggans, G., Allan, J.D., Baker, A.R., Ball, S.M., Benton, A.K., Carpenter, L.J.,
980 Commane, R., Finley, B.D., Evans, M., Fuentes, E., Furneaux, K., Goddard, A., Good, N.,
981 Hamilton, J.F., Heard, D.E., Herrmann, H., Hollingsworth, A., Hopkins, J.R., Ingham, T., Irwin,
982 M., Jones, C.E., Jones, R.L., Keene, W.C., Lawler, M.J., Lehmann, S., Lewis, A.C., Long, M.S.,
983 Mahajan, A., Methven, J., Moller, S.J., Müller, K., Müller, T., Niedermeier, N., O'Doherty, S.,
984 Oetjen, H., Plane, J.M.C., Pszenny, A.A.P., Read, K.A., Saiz-Lopez, A., Saltzman, E.S., Sander,
985 R., von Glasow, R., Whalley, L., Wiedensohler, A., Young, D.: Reactive Halogens in the Marine
986 Boundary Layer (RHaMBLe): the tropical North Atlantic experiments. *Atmos. Chem. Phys.*
987 10(3), 1031-1055, 2010.

988 G.Liebezeit, Meereschemie und globaler Wandel. In: Warnsignal Klima - Die Meere -
989 Änderungen & Risiken. Eds. J.L. Lozán, H. Graßl, L. Karbe, K. Reise, Wissenschaftliche
990 Auswertungen, Hamburg, p. 32, 2011.

991 Mahajan, A.S., Plane, J.M.C., Oetjen, H., Mendes, L., Saunders, R.W., Saiz-Lopez, A., Jones,
992 C.E., Carpenter, L.J., McFiggans, G.B.: Measurement and modelling of tropospheric reactive
993 halogen species over the tropical Atlantic Ocean. *Atmos. Chem. Phys.* 10(10), 4611-4624, 2010.

994 Mahowald, N.M., Baker, A.R., Bergametti, G., Brooks, N., Duce, R.A., Jickells, T.D., Kubilay,
995 N., Prospero, J.M., Tegen, I.: Atmospheric global dust cycle and iron inputs to the ocean. *Global
996 Biogeochem.Cy.* 19(4), 2005.

997 Mihalopoulos, N., Stephanou, E., Kanakidou, M., Pilitsidis, S., Bousquet, P.: Tropospheric
998 aerosol ionic composition in the Eastern Mediterranean region. *Tellus B* 49(3), 314-326, 1997.

999 Milton, S.F., Greed, G., Brooks, M.E., Haywood, J., Johnson, B., Allan, R.P., Slingo, A., Grey,
1000 W.M.F.: Modeled and observed atmospheric radiation balance during the West African dry
1001 season: Role of mineral dust, biomass burning aerosol, and surface albedo. *J.Geophys.Res.-
1002 Atmos.* 113, 2008.

1003 Mozurkewich, M.: Mechanisms for the Release of Halogens from Sea-Salt Particles by Free-
1004 Radical Reactions. *J.Geophys.Res.-Atmos.* 100(D7), 14199-14207, 1995.

1005 Müller, C., Iinuma, Y., Karstensen, J., van Pinxteren, D., Lehmann, S., Gnauk, T., Herrmann, H.:
1006 Seasonal variation of aliphatic amines in marine sub-micrometer particles at the Cape Verde
1007 islands. *Atmos. Chem. Phys.* 9(24), 9587-9597, 2009.

1008 Müller, K., Lehmann, S., van Pinxteren, D., Gnauk, T., Niedermeier, N., Wiedensohler, A.,
1009 Herrmann, H.: Particle characterization at the Cape Verde atmospheric observatory during the
1010 2007 RHAMBLe intensive. *Atmos. Chem. Phys.* 10(6), 2709-2721, 2010.

1011 Niedermeier, N., Held, A., Müller, T., Heinold, B., Schepanski, K., Tegen, I., Kandler, K., Ebert,
1012 M., Weinbruch, S., Read, K., Lee, J., Fomba, K.W., Müller, K., Herrmann, H., Wiedensohler, A.:
1013 Mass deposition fluxes of Saharan mineral dust to the tropical northeast Atlantic Ocean: an
1014 intercomparison of methods. *Atmos. Chem. Phys.*, 14, 2245-2266, 2014.

1015 Nunes, T., personal communication, 2013.

1016 O'Dowd, C.D. and de Leeuw, G.: Marine aerosol production: a review of the current knowledge.
1017 *Philos. T. R. Soc.A* 365(1856), 1753-1774, 2007.

1018 O'Dowd, C.D., Facchini, M.C., Cavalli, F., Ceburnis, D., Mircea, M., Decesari, S., Fuzzi, S.,
1019 Yoon, Y.J., Putaud, J.P.: Biogenically driven organic contribution to marine aerosol. *Nature*
1020 431(7009), 676-680, 2004.

1021 Ohde, T. and Siegel, H.: Biological response to coastal upwelling and dust deposition in the area
1022 off Northwest Africa. *Cont. Shelf Res.* 30(9), 1108-1119, 2010.

1023 Paatero, P.: The multilinear engine - A table-driven, least squares program for solving multilinear
1024 problems, including the n-way parallel factor analysis model, *Journal of Computational and*
1025 *Graphical Statistics*, 8, 854-888, doi 10.2307/1390831, 1999.

1026 Pavuluri, C.M., Kawamura, K., Kikuta, M., Tachibana, E., Aggarwal, S.G.: Time-resolved
1027 variations in the distributions of inorganic ions, carbonaceous components, dicarboxylic acids
1028 and related compounds in atmospheric aerosols from Sapporo, northern Japan during
1029 summertime. *Atmos. Environ.* 62, 622-630, 2012.

1030 Quinn, P.K., Charlson, R.J., Bates, T.S.: Simultaneous Observations of Ammonia in the
1031 Atmosphere and Ocean. *Nature* 335(6188), 336-338, 1988.

1032 Radhi, M., Box, M.A., Box, G.P., Mitchell, R.M., Cohen, D.D., Stelcer, E., Keywood, M.D.:
1033 Optical, physical and chemical characteristics of Australian continental aerosols: results from a
1034 field experiment. *Atmos. Chem. Phys.* 10(13), 5925-5942, 2010.

1035 Raes, F., Liao, H., Chen, W.T., Seinfeld, J.H.: Atmospheric chemistry-climate feedbacks.
1036 *J.Geophys.Res.-Atmos.* 115, 2010.

1037 Read, K.A., Mahajan, A.S., Carpenter, L.J., Evans, M.J., Faria, B.V.E., Heard, D.E., Hopkins,
1038 J.R., Lee, J.D., Moller, S.J., Lewis, A.C., Mendes, L., McQuaid, J.B., Oetjen, H., Saiz-Lopez, A.,
1039 Pilling, M.J., Plane, J.M.C.: Extensive halogen-mediated ozone destruction over the tropical
1040 Atlantic Ocean. *Nature* 453(7199), 1232-1235, 2008.

1041 Reid, E.A., Reid, J.S., Meier, M.M., Dunlap, M.R., Cliff, S.S., Broumas, A., Perry, K., Maring,
1042 H.: Characterization of African dust transported to Puerto Rico by individual particle and size
1043 segregated bulk analysis. *J.Geophys.Res.-Atmos.* 108(D19), 2003.

1044 Rijkenberg, M.J.A., Powell, C.F., Dall'Osto, M., Nielsdottir, M.C., Patey, M.D., Hill, P.G.,
1045 Baker, A.R., Jickells, T.D., Harrison, R.M., Achterberg, E.P.: Changes in iron speciation
1046 following a Saharan dust event in the tropical North Atlantic Ocean. *Mar. Chem.* 110(1-2), 56-67,
1047 2008.

1048 Rinaldi, M., Decesari, S., Carbone, C., Finessi, E., Fuzzi, S., Ceburnis, D., O'Dowd, C.D., Sciare,
1049 J., Burrows, J.P., Vrekoussis, M., Ervens, B., Tsigaridis, K., Facchini, M.C.: Evidence of a
1050 natural marine source of oxalic acid and a possible link to glyoxal. *J.Geophys.Res.-Atmos.* 116,
1051 2011.

1052 Schepanski, K., Tegen, I., Macke, A.: Saharan dust transport and deposition towards the tropical
1053 northern Atlantic. *Atmos. Chem. Phys.* 9(4), 1173-1189, 2009.

1054 Schulz, M., Prospero, J.M., Baker, A.R., Dentener, F., Ickes, L., Liss, P.S., Mahowald, N.M.,
1055 Nickovic, S., Garcia-Pando, C.P., Rodriguez, S., Sarin, M., Tegen, I., Duce, R.A.: Atmospheric
1056 Transport and Deposition of Mineral Dust to the Ocean: Implications for Research Needs.
1057 *Environ.Sci. Technol.* 46(19), 10390-10404, 2012.

1058 Sciare, J., Oikonomou, K., Cachier, H., Mihalopoulos, N., Andreae, M.O., Maenhaut, W., Sarda-

1059 Esteve, R.: Aerosol mass closure and reconstruction of the light scattering coefficient over the
1060 Eastern Mediterranean Sea during the MINOS campaign. *Atmos. Chem. Phys.* 5, 2253-2265,
1061 2005.

1062 Sciare, J., Favez, O., Sarda-Esteve, R., Oikonomou, K., Cachier, H., and Kazan, V.: Long-term
1063 observations of carbonaceous aerosols in the Austral Ocean atmosphere: Evidence of a biogenic
1064 marine organic source, *J. Geophys. Res.-Atmos.*, 114, D15302, doi:10.1029/2009jd011998, 2009.

1065 Sullivan, R.C., Guazzotti, S.A., Sodeman, D.A., Tang, Y.H., Carmichael, G.R., Prather, K.A.:
1066 Mineral dust is a sink for chlorine in the marine boundary layer. *Atmos. Environ.* 41(34), 7166-
1067 7179, 2007.

1068 Tesche, M., Gross, S., Ansmann, A., Muller, D., Althausen, D., Freudenthaler, V., Esselborn, M.:
1069 Profiling of Saharan dust and biomass-burning smoke with multiwavelength polarization Raman
1070 lidar at Cape Verde. *Tellus B* 63(4), 649-676, 2011.

1071 Tilgner, A. and Herrmann, H.: Radical-driven carbonyl-to-acid conversion and acid degradation
1072 in tropospheric aqueous systems studied by CAPRAM. *Atmos. Environ.* 44(40), 5415-5422,
1073 2010.

1074 Turpin, B.J., Saxena, P., Andrews, E.: Measuring and simulating particulate organics in the
1075 atmosphere: problems and prospects. *Atmos. Environ.* 34(18), 2983-3013, 2000.

1076 Van Pinxteren, D., Brüggemann, E., Gnauk, T., Müller, K., Thiel, C., Herrmann, H.: A GIS based
1077 approach to back trajectory analysis for the source apportionment of aerosol constituents and its
1078 first application. *J. Atmos. Chem.* 67(1), 1-28, 2010.

1079 Virkkula, A., Teinila, K., Hillamo, R., Kerminen, V.M., Saarikoski, S., Aurela, M., Viidanoja, J.,
1080 Paatero, J., Koponen, I.K., Kulmala, M.: Chemical composition of boundary layer aerosol over
1081 the Atlantic Ocean and at an Antarctic site. *Atmos. Chem. Phys.* 6, 3407-3421, 2006.

1082 Warneck, P.: In-cloud chemistry opens pathway to the formation of oxalic acid in the marine
1083 atmosphere. *Atmos. Environ.* 37(17), 2423-2427, 2003.

1084 Williams, J., de Reus, M., Krejci, R., Fischer, H., Strom, J.: Application of the variability-size
1085 relationship to atmospheric aerosol studies: estimating aerosol lifetimes and ages. *Atmos. Chem.*
1086 *Phys.* 2, 133-145, 2000.

1087 Yao, X.H., Fang, M., Chan, C.K.: Size distributions and formation of dicarboxylic acids in
1088 atmospheric particles. *Atmos. Environ.* 36(13), 2099-2107, 2002.

1089 Yao, X.H. and Zhang, L.M.: Chemical processes in sea-salt chloride depletion observed at a
1090 Canadian rural coastal site. *Atmos. Environ.* 46, 189-194, 2012.

1091

1092 Table 1: HV-Filters collected at the CVAO from 2007 to 2011.

	2007	2008	2009	2010	2011
Total amount	105	105	154	148	159
72-hour-samples	45	69	66	105	85
24-hour-samples during intensive campaigns	60	36	88	43	74
Collected at 32m	105	105	132	50	159
Collected at 4m			22	98	

1093

1094

1095

1096 Table 2 Minimum, maximum, 5 year average and standard deviations ($\mu\text{g}/\text{m}^3$) of PM_{10}
1097 aerosol components at CVAO.

Components	Min	Max	Mean	Median	Stdev
mass load	4.00	601.83	47.20	30.10	55.50
Dust	0.00	575.56	25.90	9.70	51.10
Sea salt	0.71	39.67	11.00	10.71	5.10
Cl^-	0.35	21.17	5.70	5.43	2.70
Br^-	Bdl	0.25	0.005	0.003	0.01
NO_3^-	0.14	3.76	1.10	1.00	0.60
SO_4^{2-}	0.31	7.38	2.50	2.33	1.20
$\text{C}_2\text{O}_4^{2-}$	Bdl	0.46	0.08	0.06	0.10
Na^+	0.25	12.74	3.70	3.72	1.70
NH_4^+	Bdl	0.76	0.09	0.05	0.10
K^+	Bdl	0.86	0.13	0.13	0.10
Mg^{2+}	0.05	1.34	0.40	0.37	0.20
Ca^{2+}	Bdl	4.44	0.64	0.46	0.60
OM (OC^*2)	Bdl	6.67	1.02	0.67	1.04
EC	Bdl	1.32	0.13	0.08	0.16

1098

Bdl : below detection limit.

1099 Table 3: Seasonality of PM₁₀ particle mass concentration collected with DHA-80 HV-filter
 1100 sampler between January 2007 and November 2011 on top of the tower*.

season	Mar - May	Jun – Aug	Sep – Nov	Dec - Feb	Total
Mass: >200 µg/m ³	2	0	1	15	18
Mass: 90-200 µg/m ³	7	4	10	22	43
Mass: 20-90 µg/m ³	62	98	91	98	349
Mass: <20 µg/m ³	47	22	19	41	129
Total samples	118	124	121	176	539

1101 *Samples collected between 23rd of October 2009 and 09th of July 2010 were not included here
 1102 because of the lower sampling height on the container roof.

1103

1104 Table 4: Comparison of published averaged oxalate concentration in PM₁₀ aerosols with
 1105 the results of this study

Sampling site	Sampling interval	Oxalate [µg/m ³]	Reference
CVAO, marine non-polluted	Winters 2007-2011	0.07±0.06	This study
CVAO, marine non-polluted	Summers 2007-2011	0.06±0.05	This study
CVAO, continentally influenced	2007-2011	0.12±0.06 (Africa) 0.12±0.05 (Europe)	This study
Amsterdam Island	2003-2007	0.0003 – 0.017	
Mace Head	2006	0.0027 – 0.039	(Rinaldi et al. 2011)
Tropical to Northwest Pacific	Sep-Dec 1990	0.040	(Kawamura and Sakaguchi 1999)
Tropical Atlantic	April 1996	0.052±0.030	(Johansen et al. 2000)
Atlantic Ocean 25°N - 4°S	November 1999	0.074±0.048	(Virkkula et al. 2006)
Hong Kong	December 2000	0.35	(Yao et al. 2002)
Sapporo , Japan	August 2005	0.196	(Pavuluri et al. 2012)

1107 Table 5: Comparison of major non-sea-salt components and halogenide depletion (mean
 1108 values and standard deviation as an estimation of the scatter) in four classes of
 1109 particulate matter collected at the tower at the CVAO.

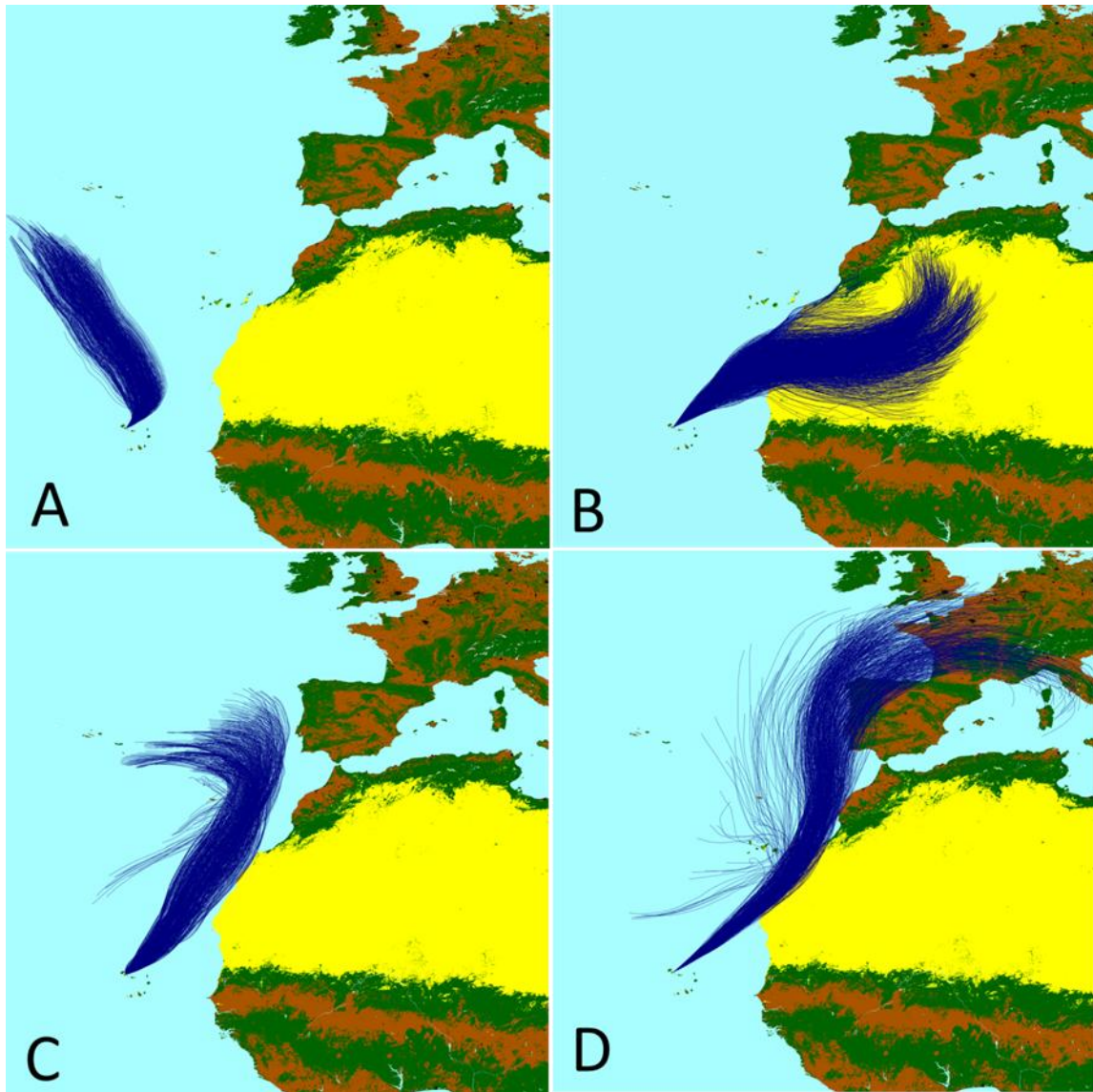
1110

Concentration [$\mu\text{g}/\text{m}^3$]	Dust – rich Saharan aerosol	Marine aerosol summer	Marine aerosol Winter	Europe influenced aerosol	Mean of all samples
Mass concentration (N)	173.4 \pm 95.5 (56)	16.4 \pm 4.5 (43)	14.5 \pm 5.8 (33)	35.3 \pm 13.6 (55)	47.3 \pm 55.5 (539)
Dust (estimated)	144.6 \pm 95.8	2.7 \pm 2.6	2.0 \pm 4.1	6.1 \pm 9.9	25.8 \pm 51.4
OM	3.16 \pm 1.69	0.58 \pm 0.35	1.04 \pm 0.7	0.86 \pm 0.47	1.01 \pm 1.04
EC	0.38 \pm 0.32	0.05 \pm 0.05	0.04 \pm 0.03	0.12 \pm 0.08	0.13 \pm 0.16
Nitrate	1.75 \pm 0.69	0.58 \pm 0.28	0.48 \pm 0.22	1.36 \pm 0.49	1.10 \pm 0.56
Non-sea-salt Sulfate	2.46 \pm 1.05	1.01 \pm 0.45	0.47 \pm 0.31	1.76 \pm 0.99	1.54 \pm 1.04
Ammonium	0.064 \pm 0.08	0.07 \pm 0.05	0.036 \pm 0.	0.165 \pm 0.18	0.088 \pm 0.10
Time over Ocean [h]	<48	>120	>120	>72	--
Chloride depletion [%]	8.8 \pm 8.5	26 \pm 15	20 \pm 13	30 \pm 12	16 \pm 10
Bromide depletion [%]	62 \pm 42	88 \pm 13	83 \pm 20	87 \pm 11	80 \pm 20
$[\text{Cl}^-] / [\text{Na}^+]$ (1.17 in sea water)	1.06	0.95	1.03	0.80	
$[\text{Cl}^- + \text{NO}_3^-] / [\text{Na}^+]$	1.19	1.02	1.10	0.91	

1111

1112

1113
1114

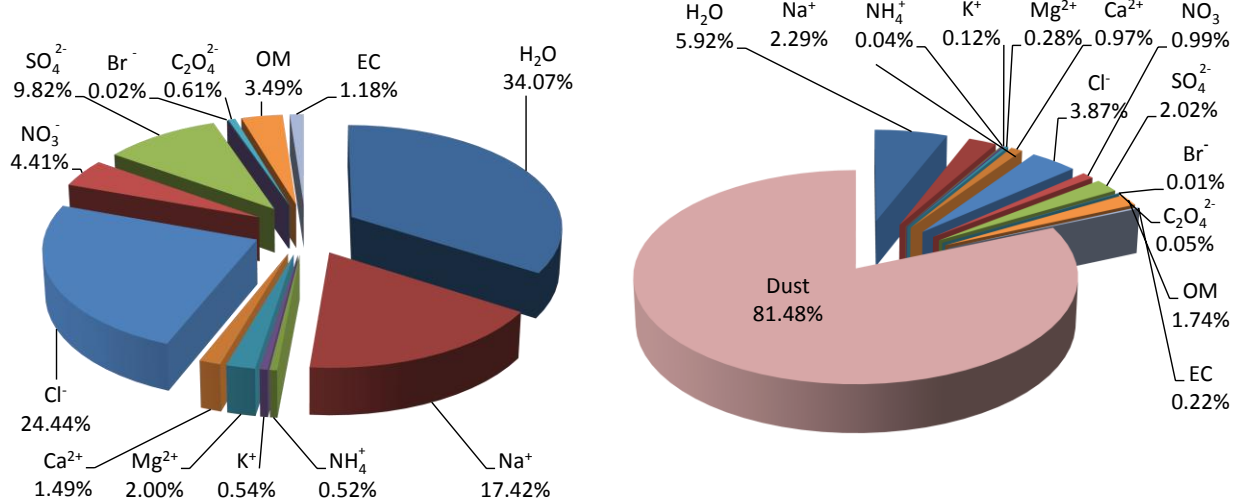


1115

1116

1117 Figure 1. Typical 96 hour air mass back trajectory ensembles calculated for CVAO during the
1118 routine filter sampling periods, aerosol type and PM_{10} mass concentration are given in
1119 parentheses: A) 02-May-2011: marine air mass from Northern Atlantic Ocean (mass, $m=8.28$
1120 $\mu g/m^3$); B) 14-Jan-2011: Saharan air mass (dust loaded, $m=155.04 \mu g/m^3$); C) 12-Jul-2008:
1121 slightly polluted air mass from the Northwest-African coast and the Canary Islands, $m=21.61$
1122 $\mu g/m^3$. D) 02-Feb-2011: Air mass from Europe crossing the coast-line of NW Africa and the
1123 Canary Islands (anthropogenically influenced, $m=64.89 \mu g/m^3$);

1124



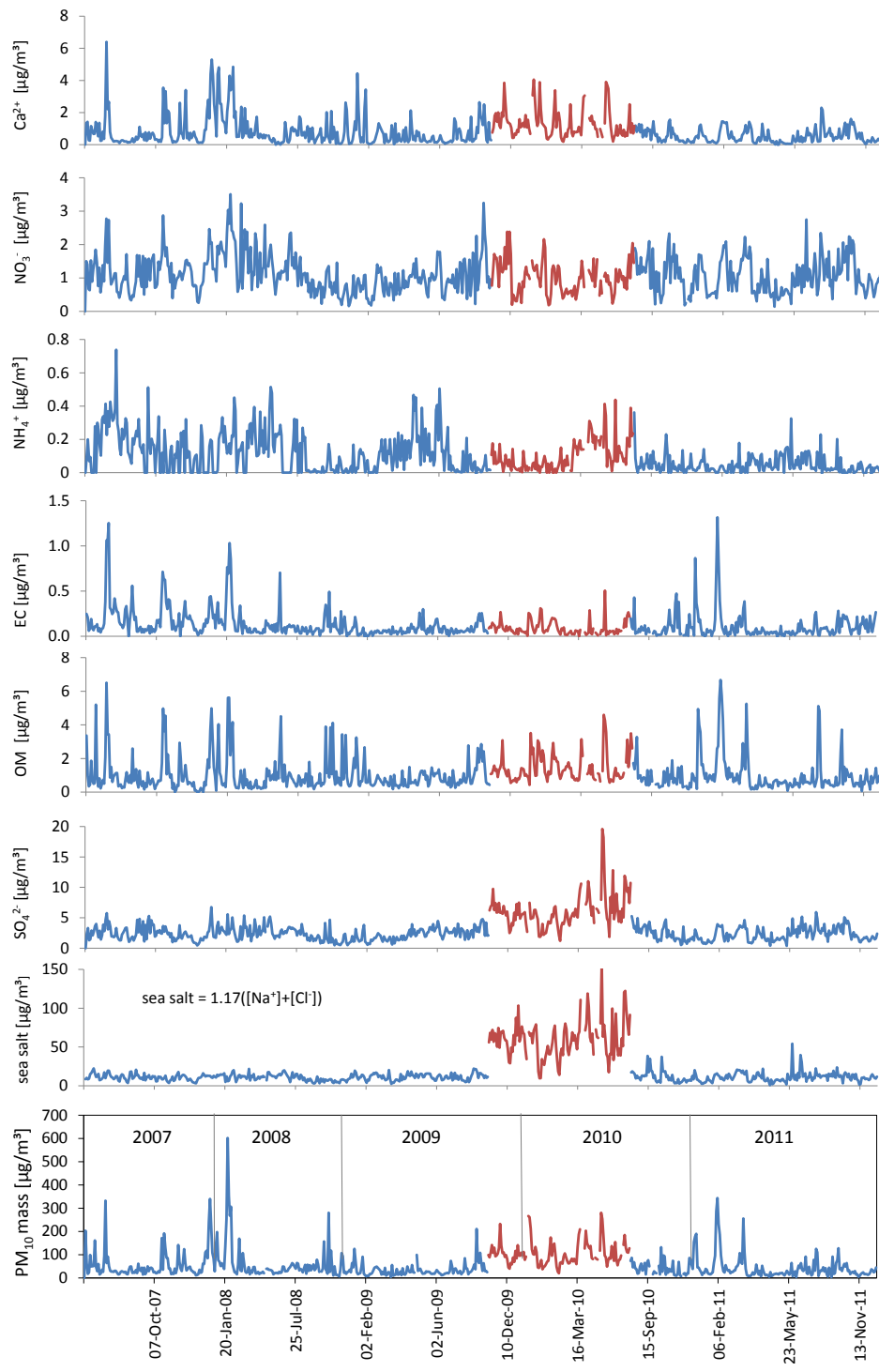
1125

1126

1127 Figure 2. Averaged PM_{10} constitution for 183 marine samples (left) and 49 mineral dust
1128 dominated aerosol samples (right) collected at 32 m on top of the tower.

1129

1130

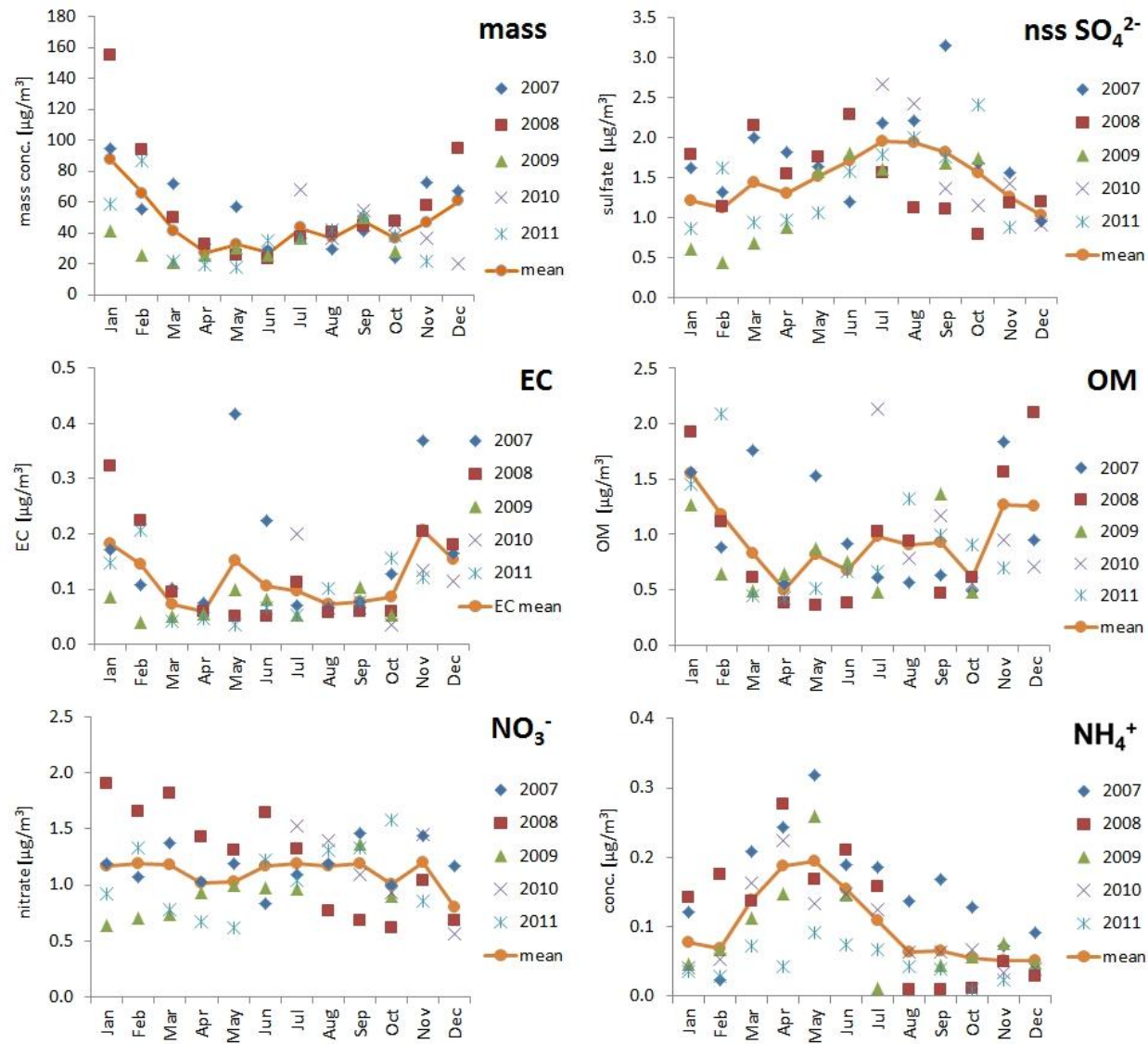


1131

1132 Figure 3. Time series of mass concentration and major PM₁₀ aerosol components in filter samples
 1133 collected during the five years from 2007 to 2011. During the period from 23 October 2009 till
 1134 09 July 2010 (red line) all samples were collected on top of a storage container with an inlet
 1135 height of 4 m above ground, all other samples were collected on top of the tower with an inlet
 1136 height of 32m above ground.

1137

1138



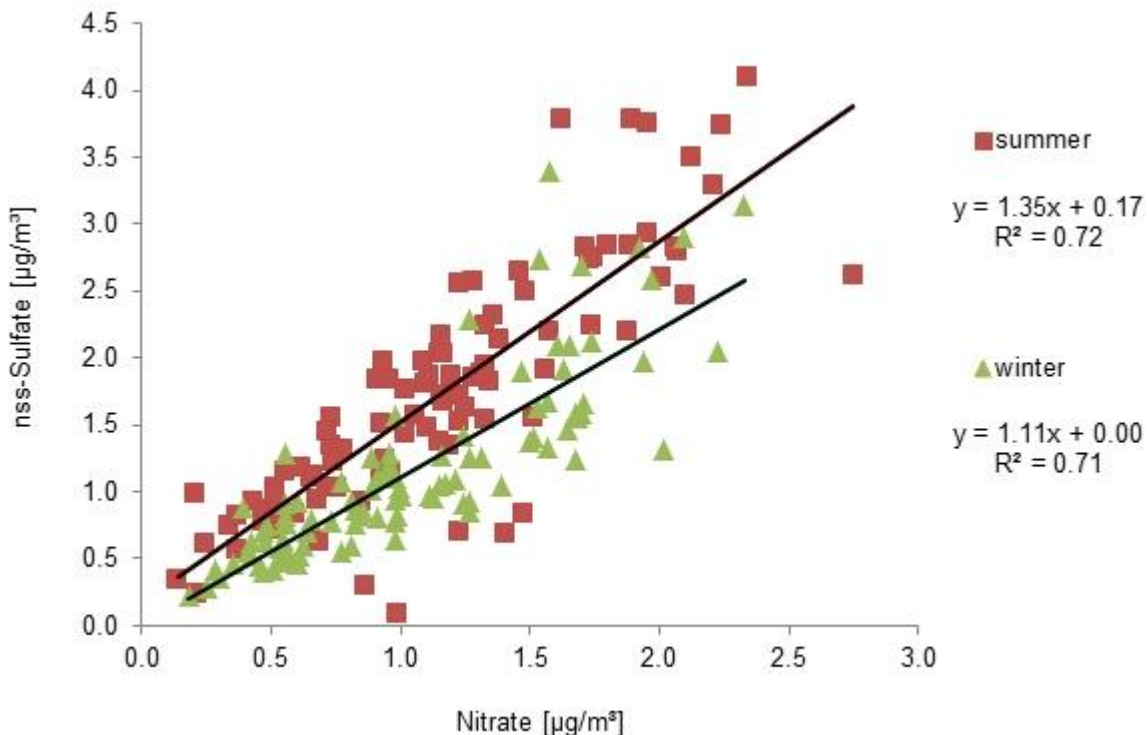
1139

1140

1141 Figure 4. Annual variability and monthly mean of PM₁₀ mass concentration, non-sea-salt sulfate,
 1142 elemental carbon (EC), organic matter (OM), nitrate, and ammonium during the five years of
 1143 measurements for samples collected on the tower.

1144

1145



1146

1147

1148 Figure 5. Correlation between nitrate and nss-sulfate between Summer and Winter in samples
 1149 collected from July 2010 to November 2011.

1150

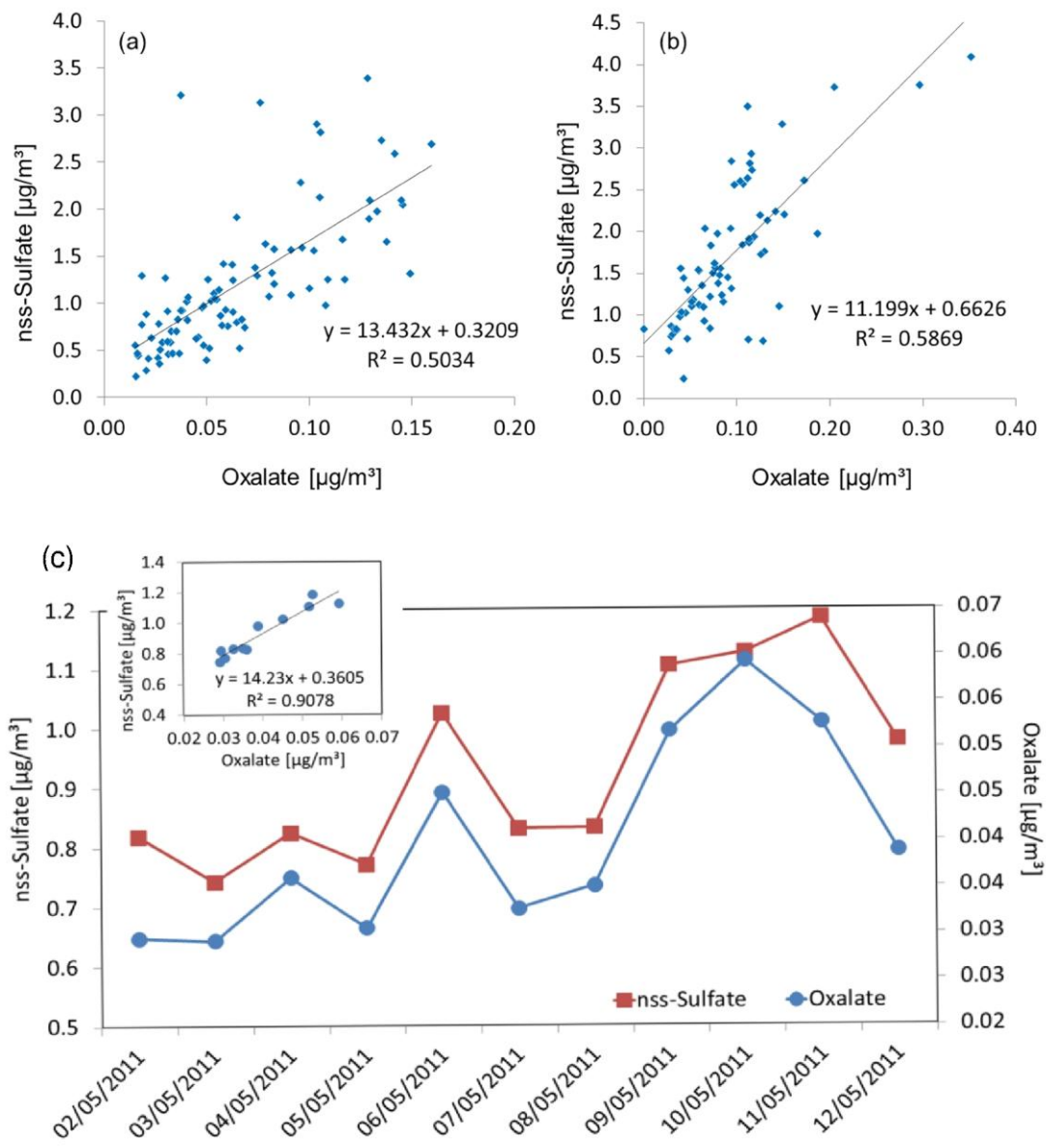
1151

1152

1153

1154

1155



1156

1157

1158

Figure 6. Correlation between nss-sulfate and oxalate in filter samples during 2010/2011, above
1159 (a) winter, (b) summer, and below (c) concentration and correlation during a marine clean air
1160 episode in May 2011.

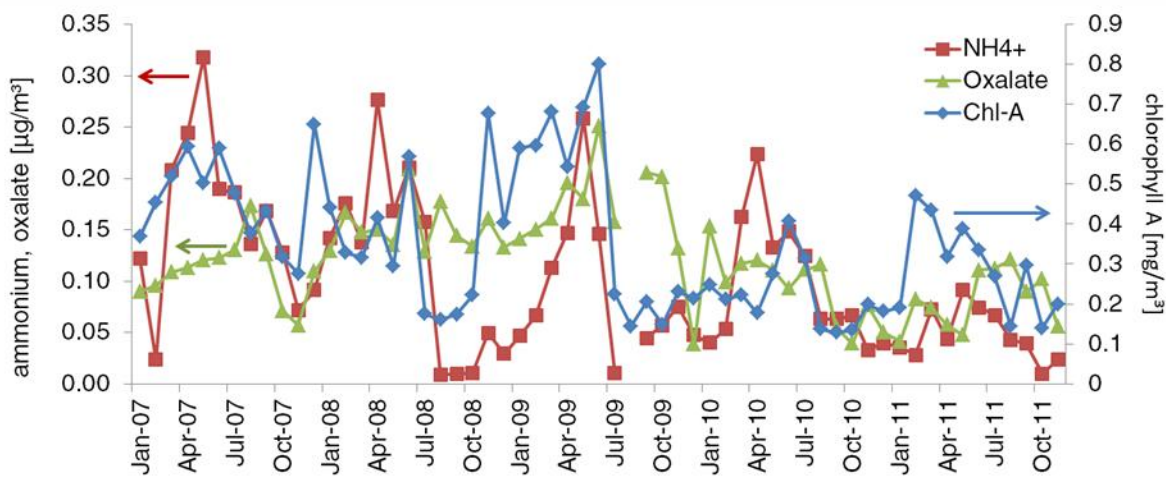
1161

1162

1163

1164

1165



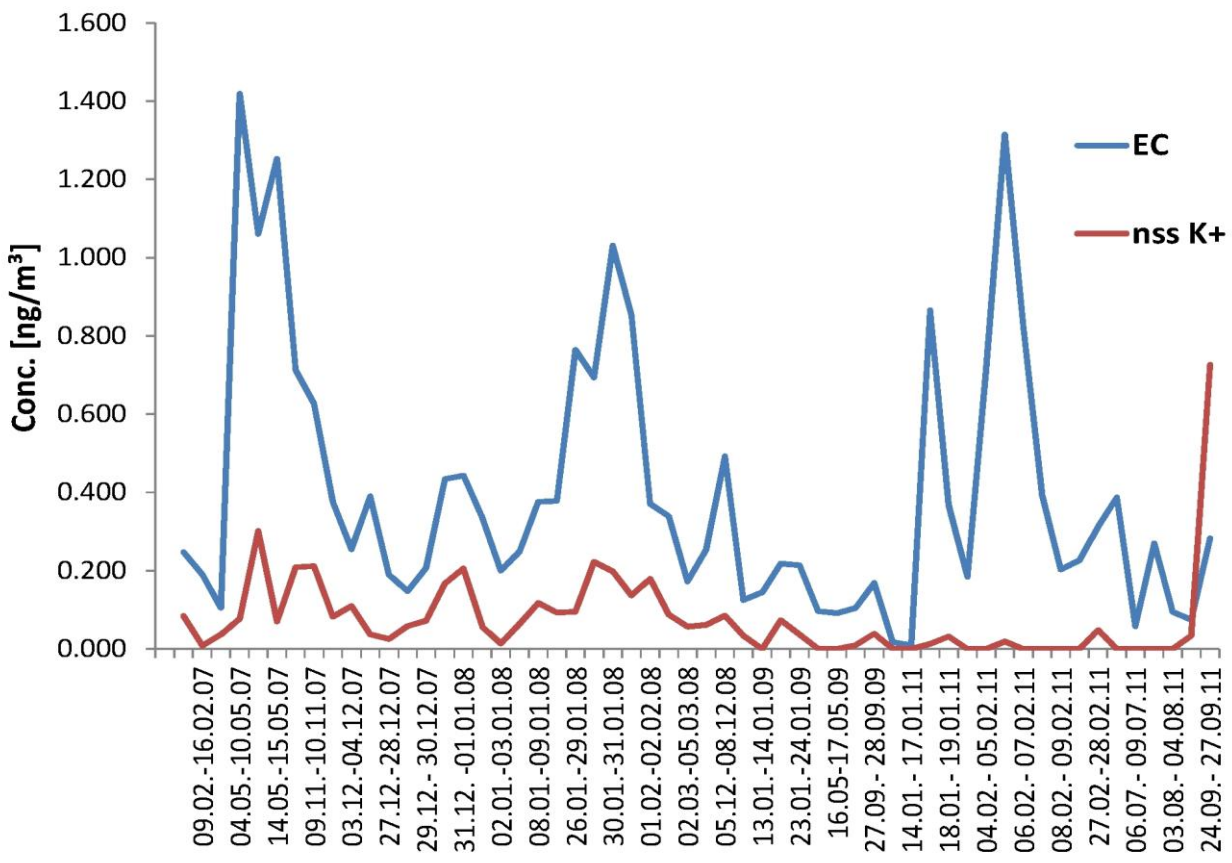
1166

1167

1168 Figure 7. Monthly mean of chlorophyll A in the tropical NE Atlantic (selected area for averaging:
1169 Lat(16.985, 24.895), Lon(-24.87, -18.278)), oxalate and ammonium in PM_{10} aerosol samples
1170 collected at the CVAO.

1171

1172

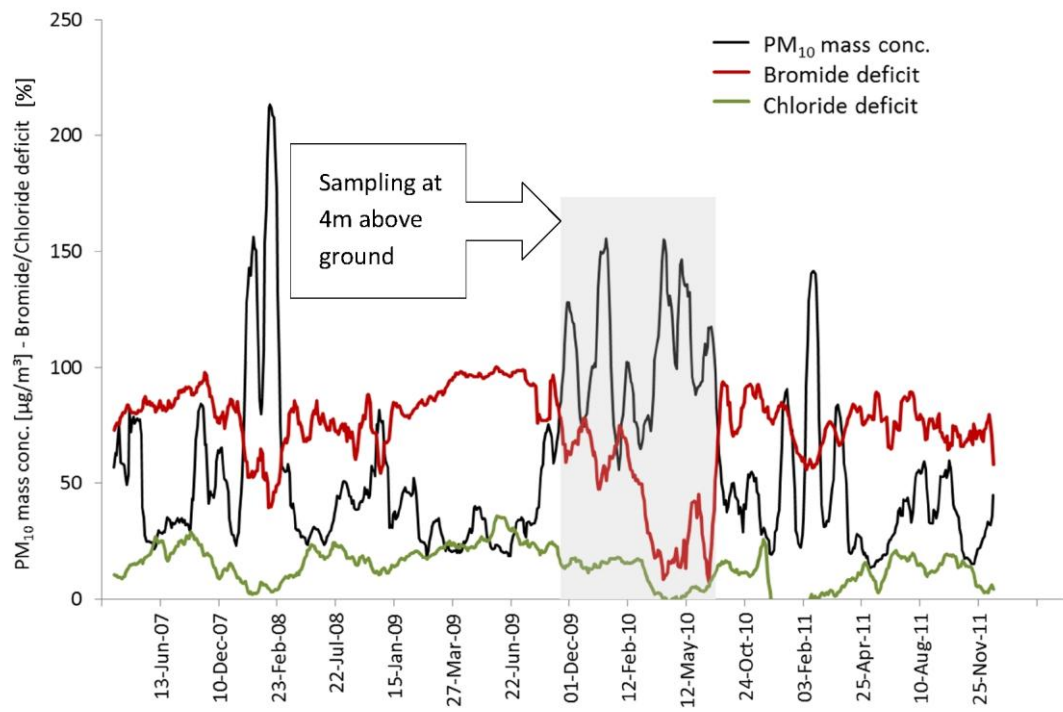


1173

1174

1175 Figure 8. Time series of nss-potassium (nss-K⁺) and elemental carbon (EC) measured during air
1176 mass inflow from Africa revealing similar temporal variations.

1177



1178

1179

1180

1181

1182

1183

1184

1185

1186

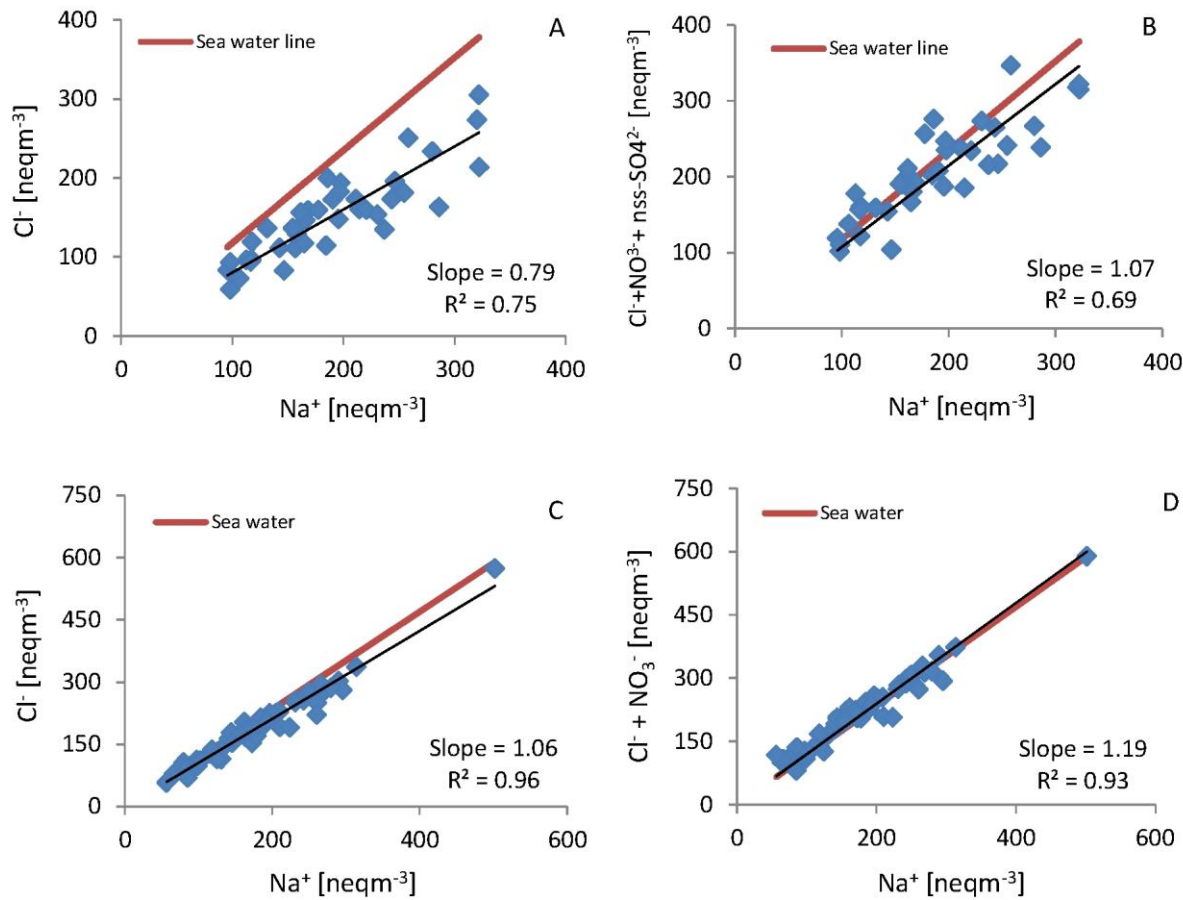
1187

1188

1189

1190

Figure 9. Variability of bromide and chloride deficit in comparison to the total PM₁₀ mass concentration (all curves represent 10-samples running means) and the season.



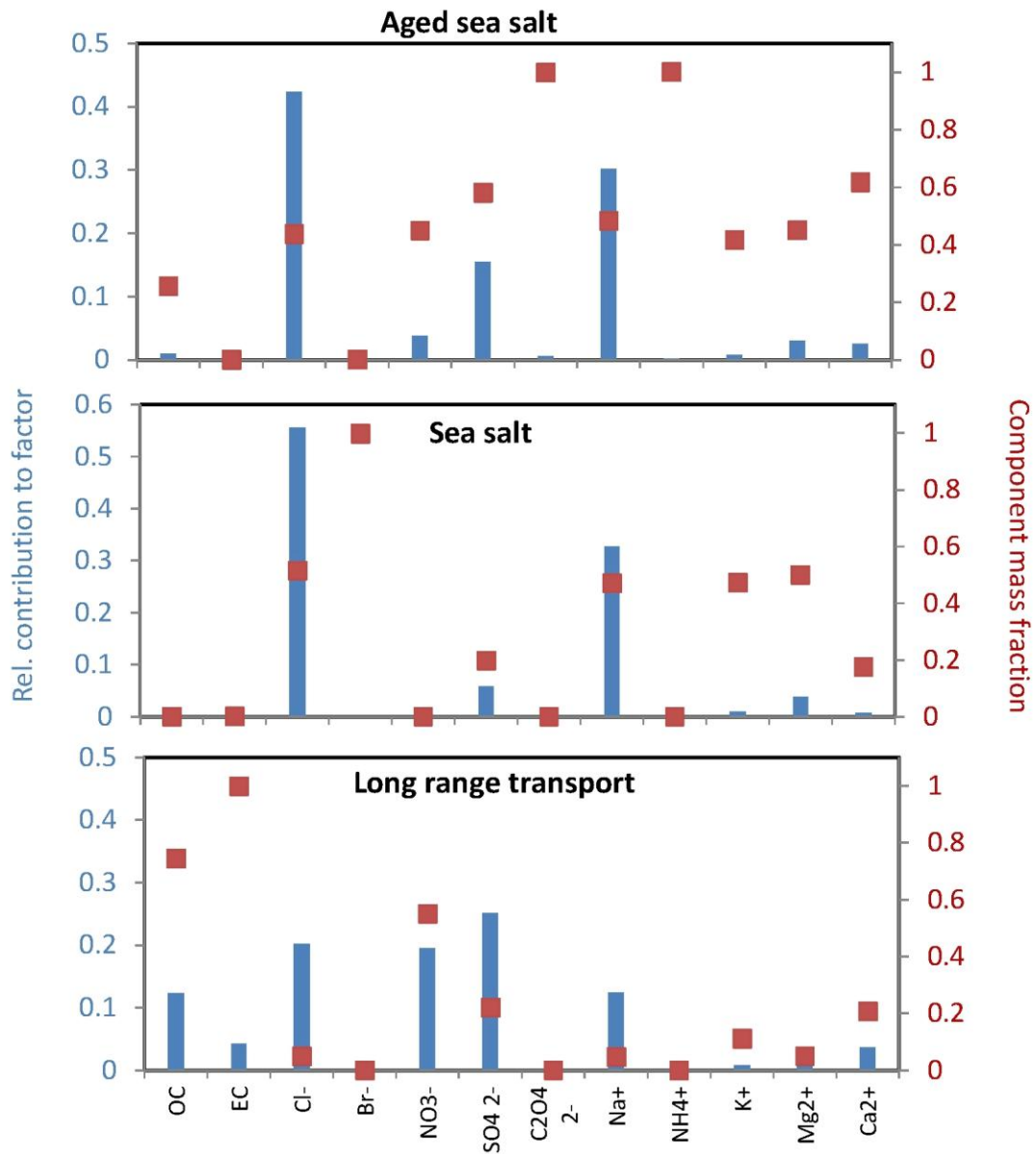
1191

1192

1193 Figure 10. Scatter plots between a) Na^+ and Cl^- , b) Na^+ and $\text{Cl}^- + \text{NO}_3^- + \text{nss-SO}_4^{2-}$ during summer
 1194 marine air mass inflow and c) Na^+ and Cl^- , d) Na^+ and $\text{Cl}^- + \text{NO}_3^-$ during Saharan dust events at
 1195 the CVAO.

1196

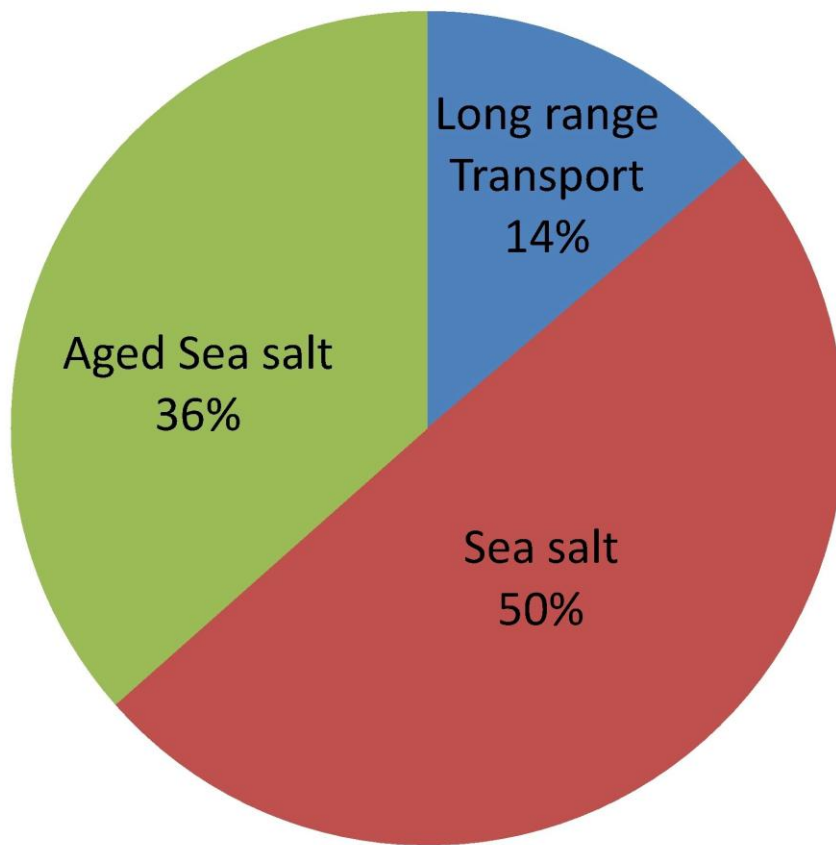
1197



1198
1199
1200
1201
1202
1203
1204
1205
1206

Figure 11. Source profiles identified from measured PM₁₀ components at CVAO. Results are from 671 analyzed filters. The relative contribution of each species to a given factor is represented as blue bars while the relative contribution of each factor to the total species concentration is represented as red square (right axis).

1207



1208

1209

1210 Figure 12. Average contribution of each source to the total analyzed species

1211

1212

1213

1214

1215

1216